U.S. DEPARTMENT OF ENERGY | Office of NUCLEAR ENERGY

ASI Advanced Sensors and Instrumentation

INL/MIS-24-81764

Optimal Sparse Sensing and Sparse Learning for Nuclear Digital Twins

Mohammad G. Abdo,
Digital Reactor Technology and Development C160, INL

Advanced Sensors and Instrumentation (ASI) Annual Program Webinar
November 4, 6-7, 2024

Modeling and Simulation Specialist: Mohammad Abdo, Ph.D.

Digital Reactor Technology and Development C160, INL

About the Presenter

- Mohammad G. Abdo, Modeling and Simulation Specialist,

  Digital Reactor Technology and Development (C160).

  Reactor Systems Design and Analysis | NS&T | INL

- Research areas of interest and highlights:
  - Sensitivity-informed ROM-based pre-conceptual design of a TREAT Sodium Loop experiment.
  - LWRS-RISA pathway: Fuel reload pattern Optimization. (**AI technical lead and WPM**)
  - Validation, Scaling, and Interpolation of experiments for representativity of full plants. (**PI**)
  - Optimal Sparse Sensing and Sparse Signal Recovery for Nuclear Digital Twins. (**PI**)
  - Metamodeling for predicting effective properties of porous materials (TRISO compacts). (**PI**)
  - Multiresolution analysis of time-series signals for optimal dispatching of Integrated Energy Systems.
  - **Areas of interest**: Machine Learning, Deep Learning, Reduced Order Modeling, SA/UQ, Sparse Sensing/learning, Digital Twinning, Koopman theory, time delayed embeddings for digital signal processing, Operator Learning (Fourier Neural Operators, Physics-informed Deep-ONETs,..), NLP, Transformers, Attention Mechanisms, LLMs, RAGs, CoT, ToT, MoE, AI Agents and more.

Project Overview

Enable sparse sensing and sparse learning in nuclear digital twins through reconstruction of reactor core flow fields, using optimal sensor placement with spatial constraints.

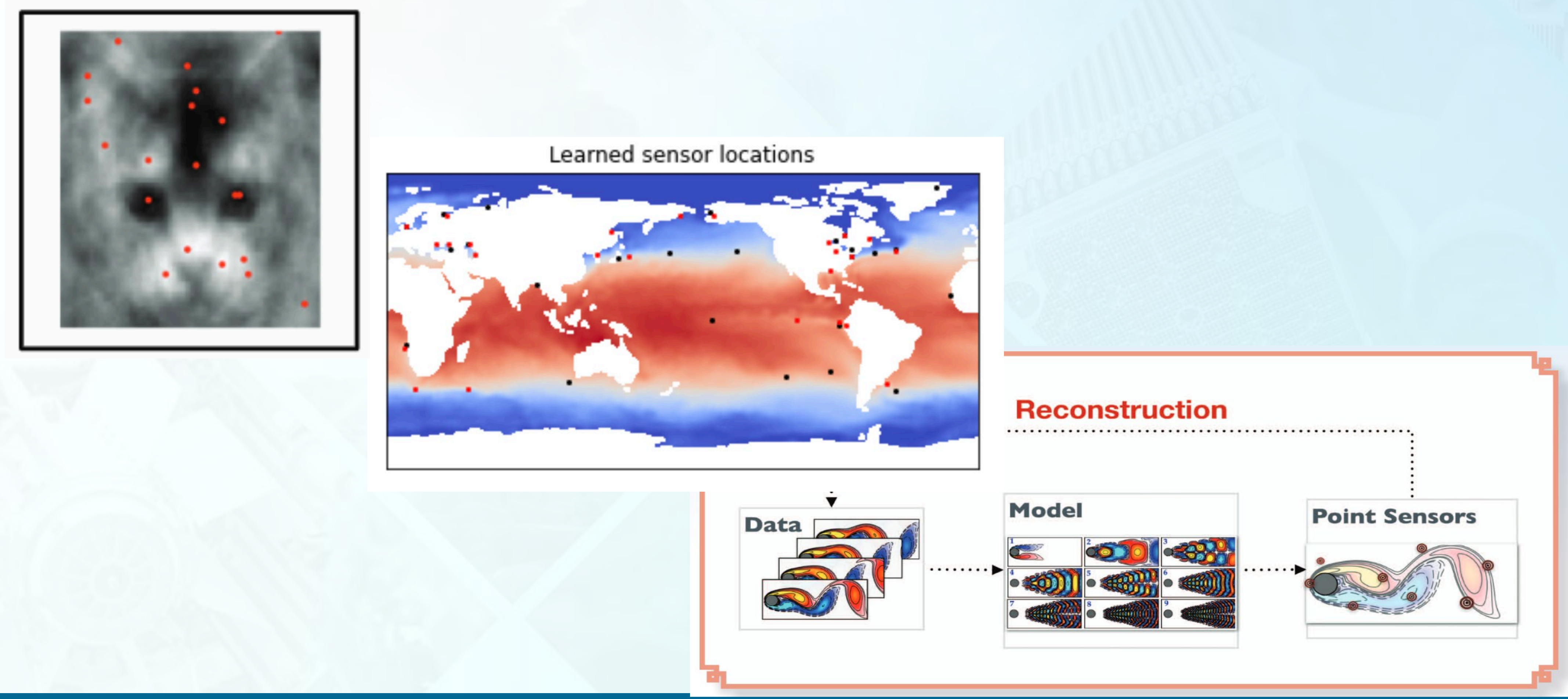

Project Overview

@Team

INL:

Mohammad G Abdo: PI

Pattrick Calderoni: Co-PI

Joshua Cogliati: Co-PI

Richard Skifton

Carlos Perez

JunSoo Yoo

UW:

Krithika Manohar: Co-PI

Steven Brunton: Co-PI

Niharika Karnik: Ph.D. Student

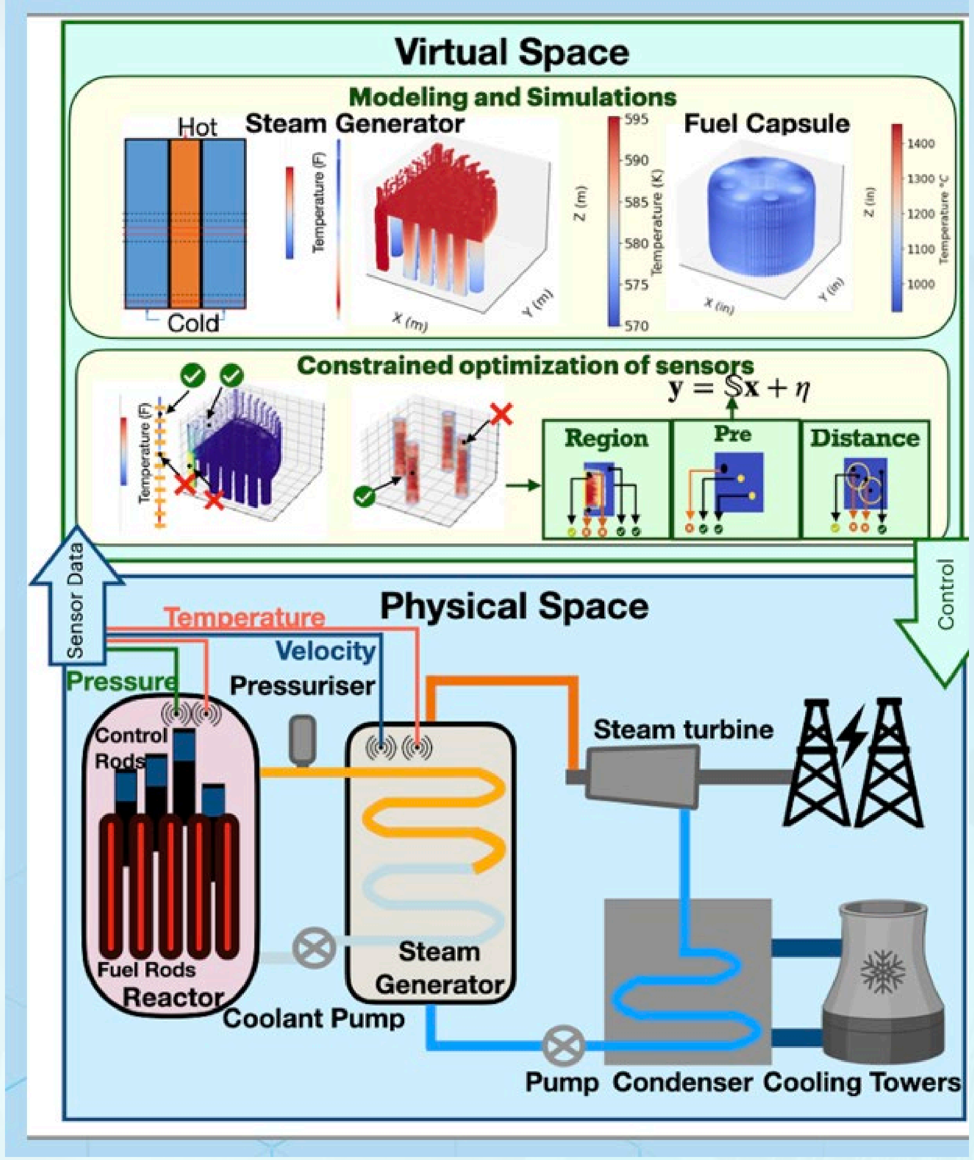

What is a digital Twin?

A digitized replica of a physical component, system, or process rendering its whole lifecycle utilizing connectivity to real-time sensory data alongside deep analytics (ML/DL/AI) that :

- enables adaptive learning, inference, reasoning, and decision-making with minimal human intervention
- to achieve the ultimate goal of facilitating real, continuous, and dynamic communication between design, manufacturing, and quality

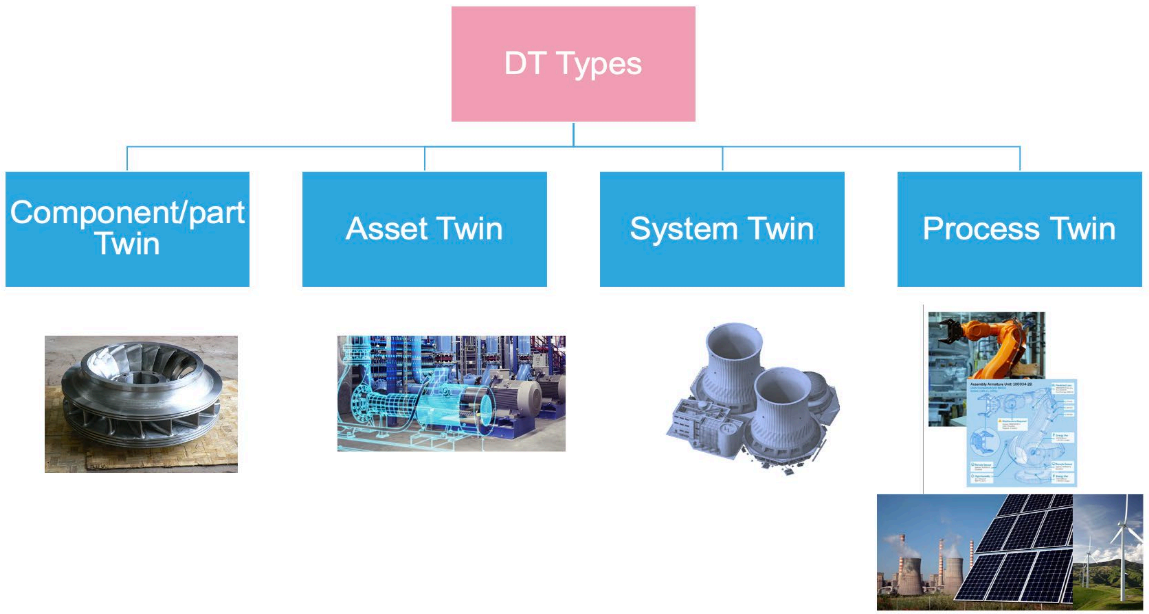

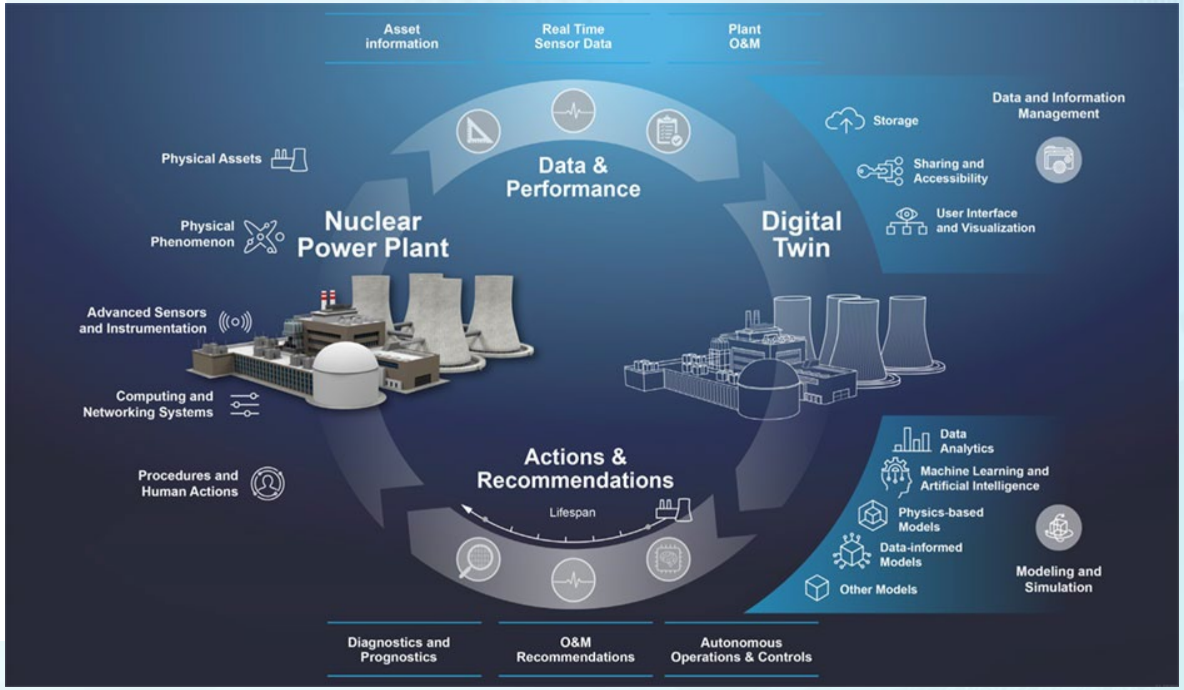

Source: https://www.nrc.gov/reactors/power/digital-twins.html

Diagram courtesy: Idaho National Laboratory (INL)

DT requirements

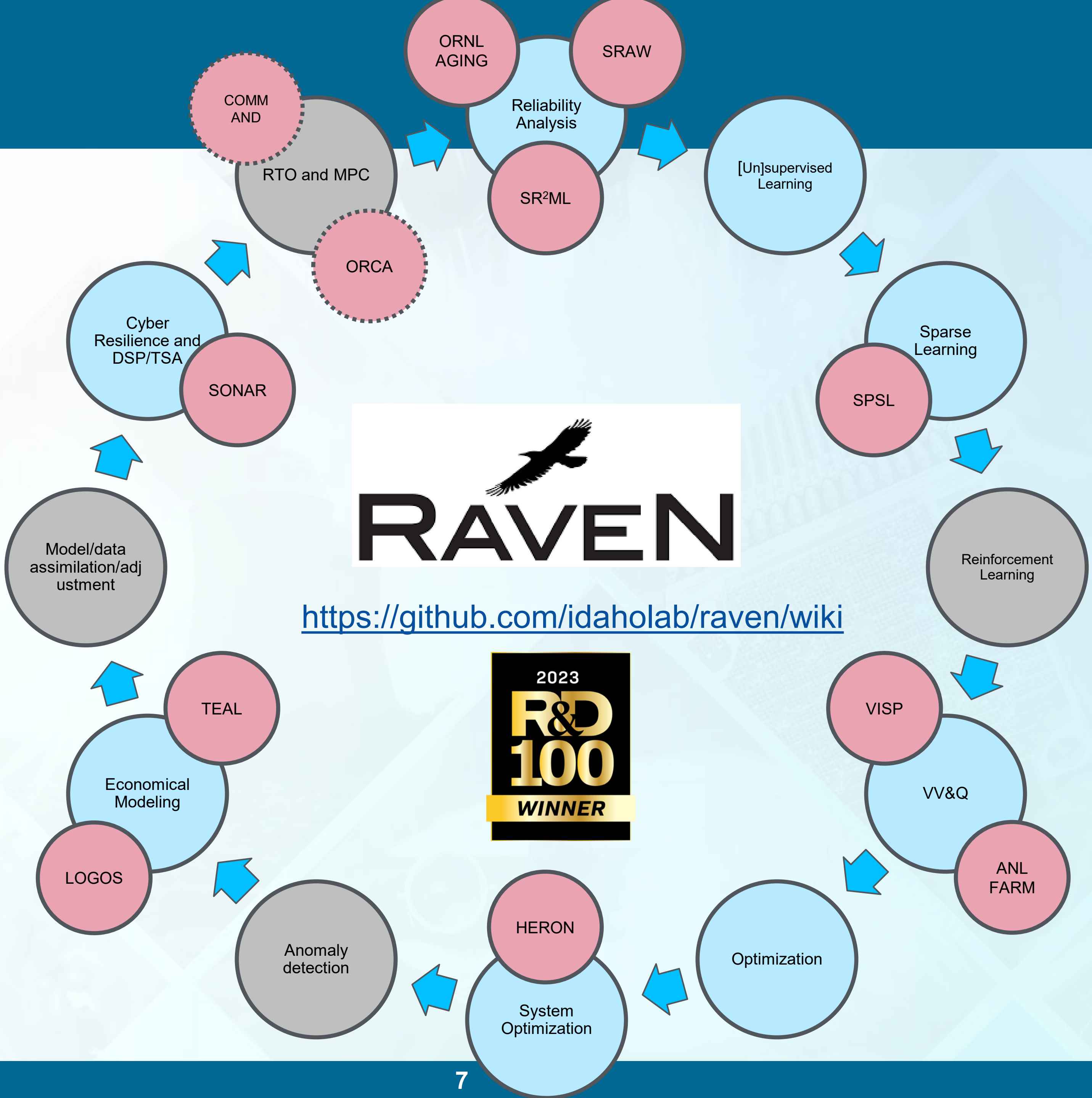

Core Capability

RAVEN Plugin

Future capability

Future connection

Technology Impact

- The methodology and algorithms are modular and agnostic of the application.
  - Customers: Every entity that uses instrumentation (power plants, utilities, vendors, testing regs, universities running experimental facilities, TREAT, Microreactors, etc.)
  - When deployed it facilitates:
    - Reconstruction of full fields of interest from few measurements.
    - All other reconstructed points can serve as virtual sensors especially for unreachable locations.
    - Will provide the minimal number of sensors and their optimal placement for reconstruction, forecasting, classification and off-normal conditions detection.
    - Several upstream and downstream components can communicate creating a network of digital Twins.
    - This paves the road for the sought digital transformation and seamlessly facilitate the communication between Integrated energy systems encompassing nuclear and renewable energy.

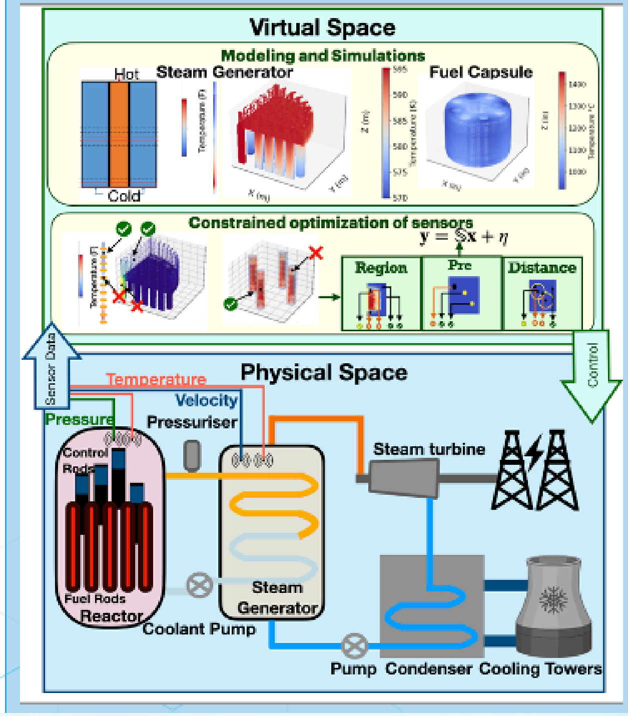

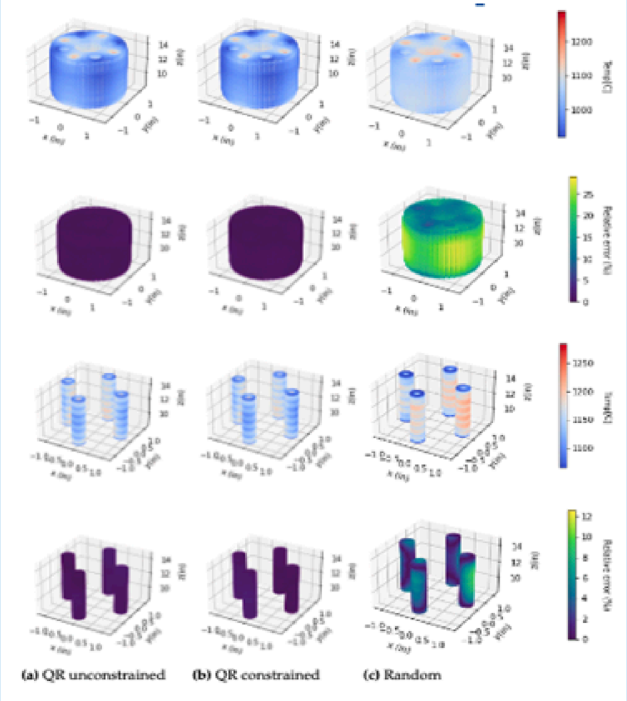

Results - Case Study 1: OPTI-Twist Prototype

GOAL: Reconstruct temperature profile with minimal sensors under :

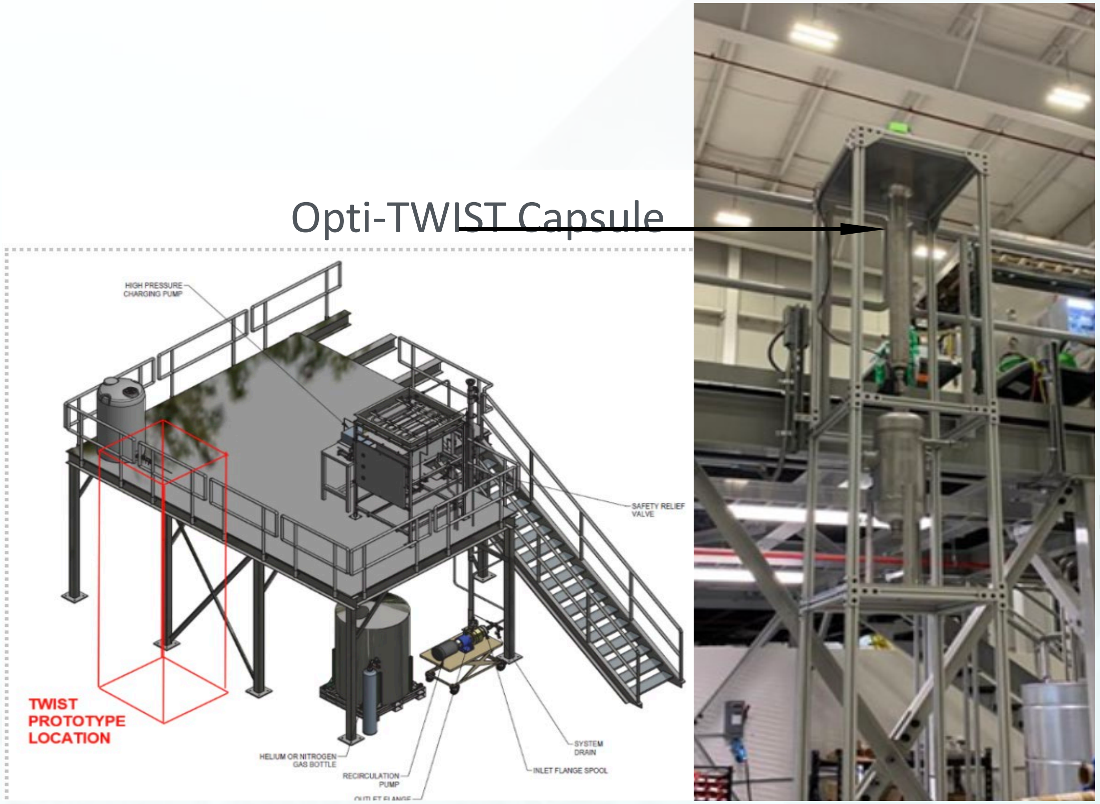

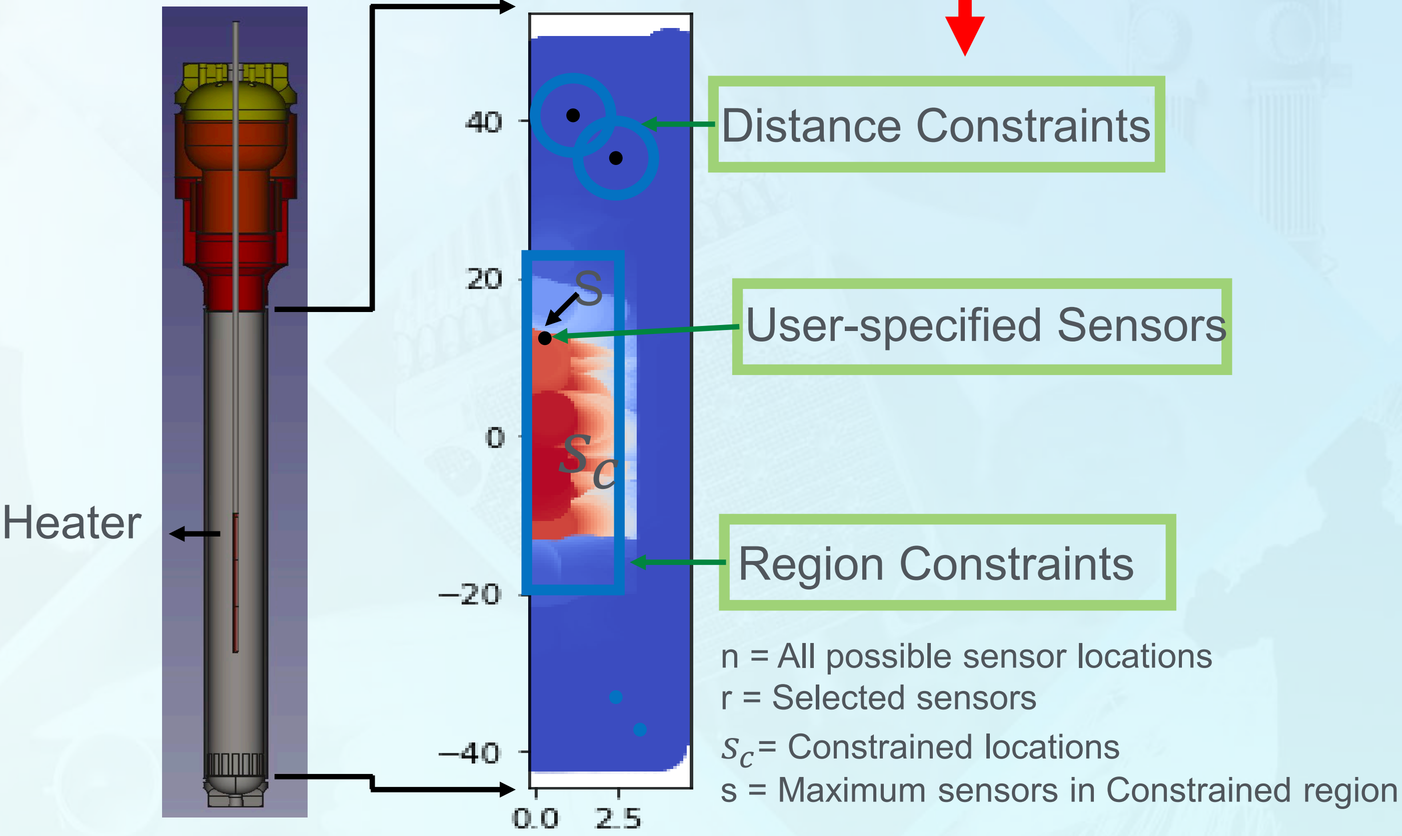

Model Calibration Experiment(s)

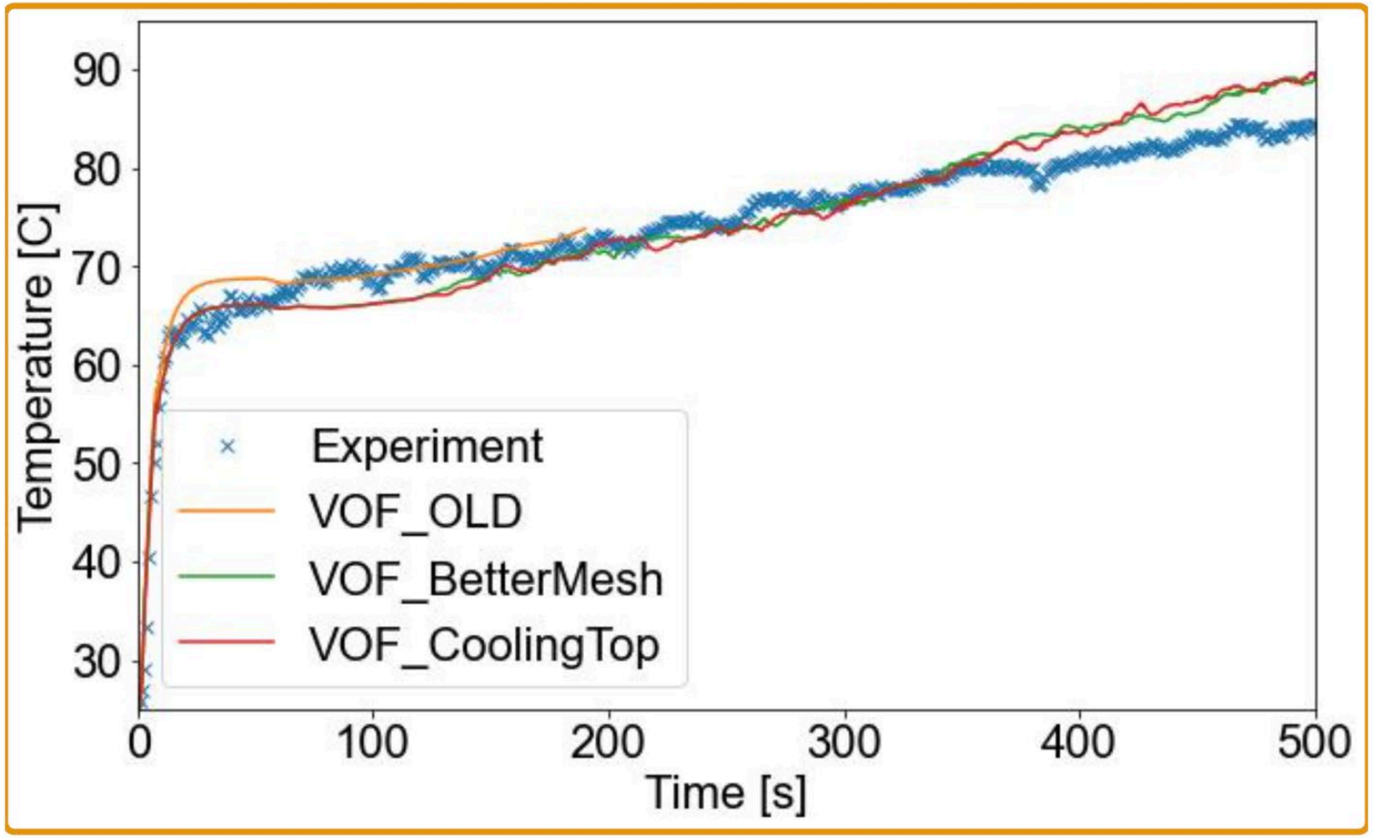

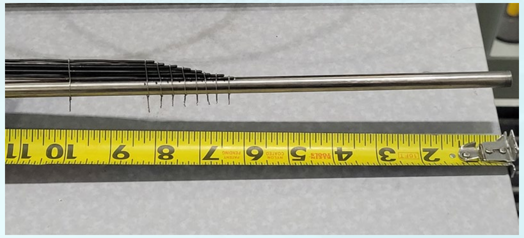

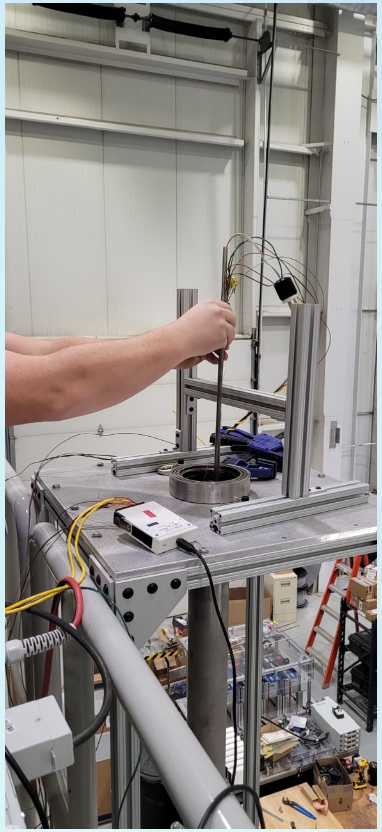

Uniformly Placed Thermocouples

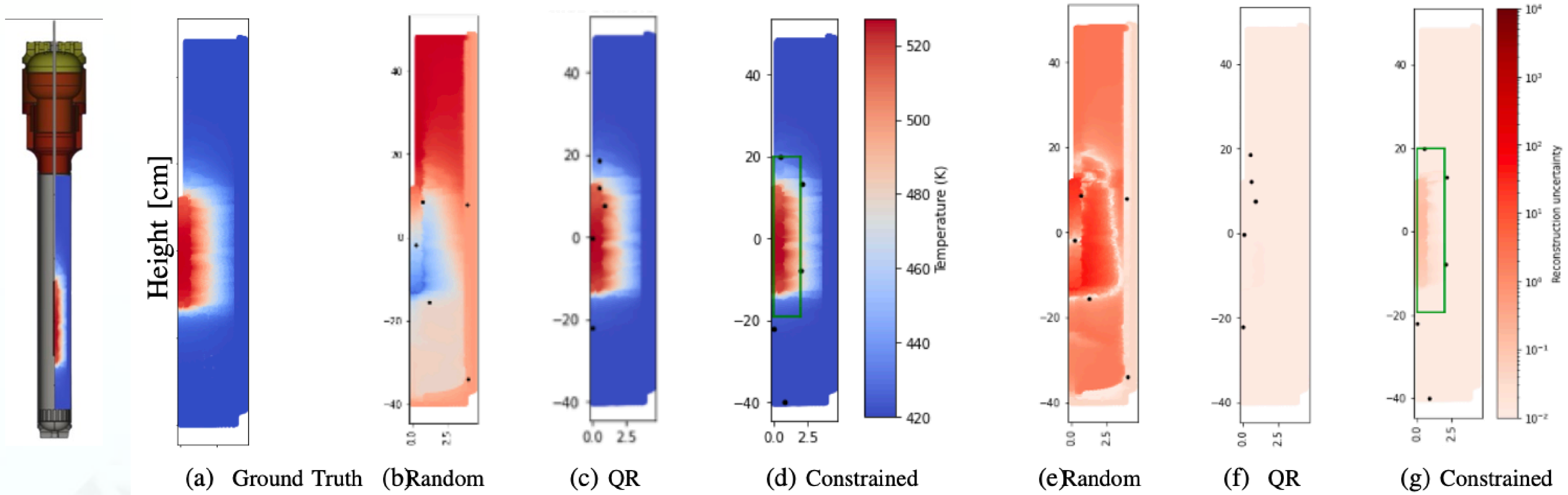

OPTI-TWIST temperature profile reconstructions through different sensor layouts and uncertainty in estimation caused by noisy sensor measurements. Unconstrained optimization places sensors near the heater region (c), resulting in highly accurate reconstruction with $\epsilon = 0.168$ (a), with constrained optimized sensors resulting in comparably high accuracy $\epsilon = 0.174$ (d). Random sensor placement (b) results in inaccurate reconstructions ($\epsilon = 25.24$) and large estimation uncertainty (e) compared to that of optimized sensor locations (f,g).

- Reconstruction error decreases with more optimized sensors (unconstrained or constrained)
- Random placements still suffer from high error even with additional sensors.

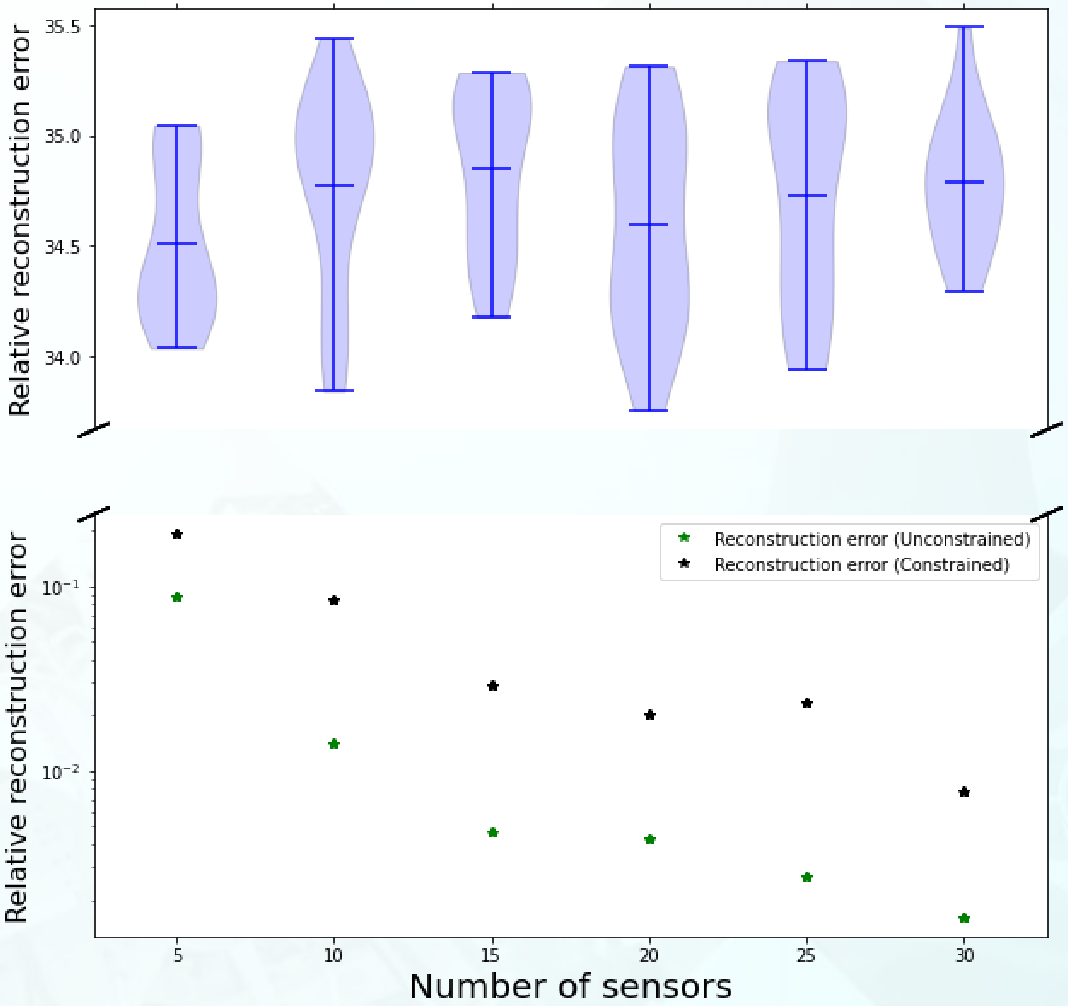

RAVEN

```xml
<Models>
  <PostProcessor name="mySPSL" subType="SparseSensing" verbosity="debug">
    <Goal subType="reconstruction">
      <features>X (m),Y (m),Temperature (K)</features>
      <target>Temperature (K)</target>
      <basis>SVD</basis>
      <nModes>4</nModes>
      <nSensors>4</nSensors>
      <optimizer>QR</optimizer>
    </Goal>
  </PostProcessor>
</Models>
```

Implemented in RAVEN (INL's Open-source ML pipeline orchestrator)

Results - Case Study 2: TRISO Fuel Irradiation Experiment

- Goal 1 : Optimize height (Z-axis) at which thermocouples should be placed inside the fuel to reconstruct fuel temperature profile.
- Goal 2 : Choose best thermocouple locations on the graphite holder from all the green holes shown in Figure 1 to reconstruct the fuel temperature profile.

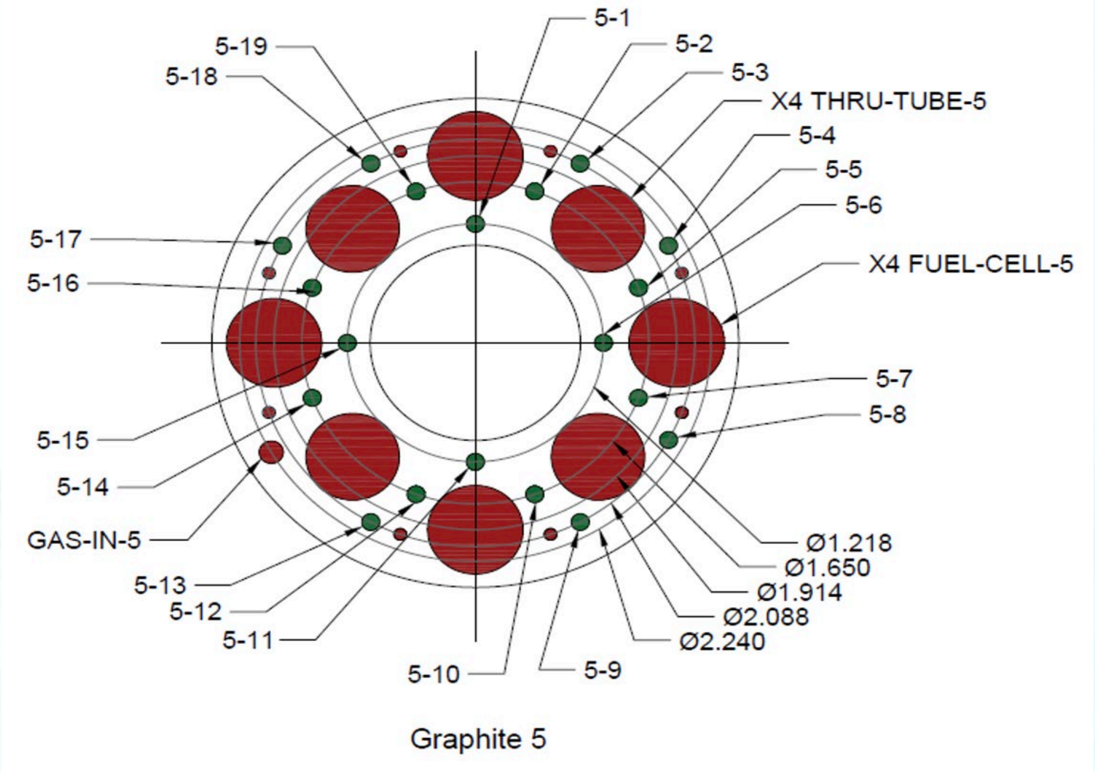

Figure 1 : Top view of Graphite Holder 5 with thermocouple locations.

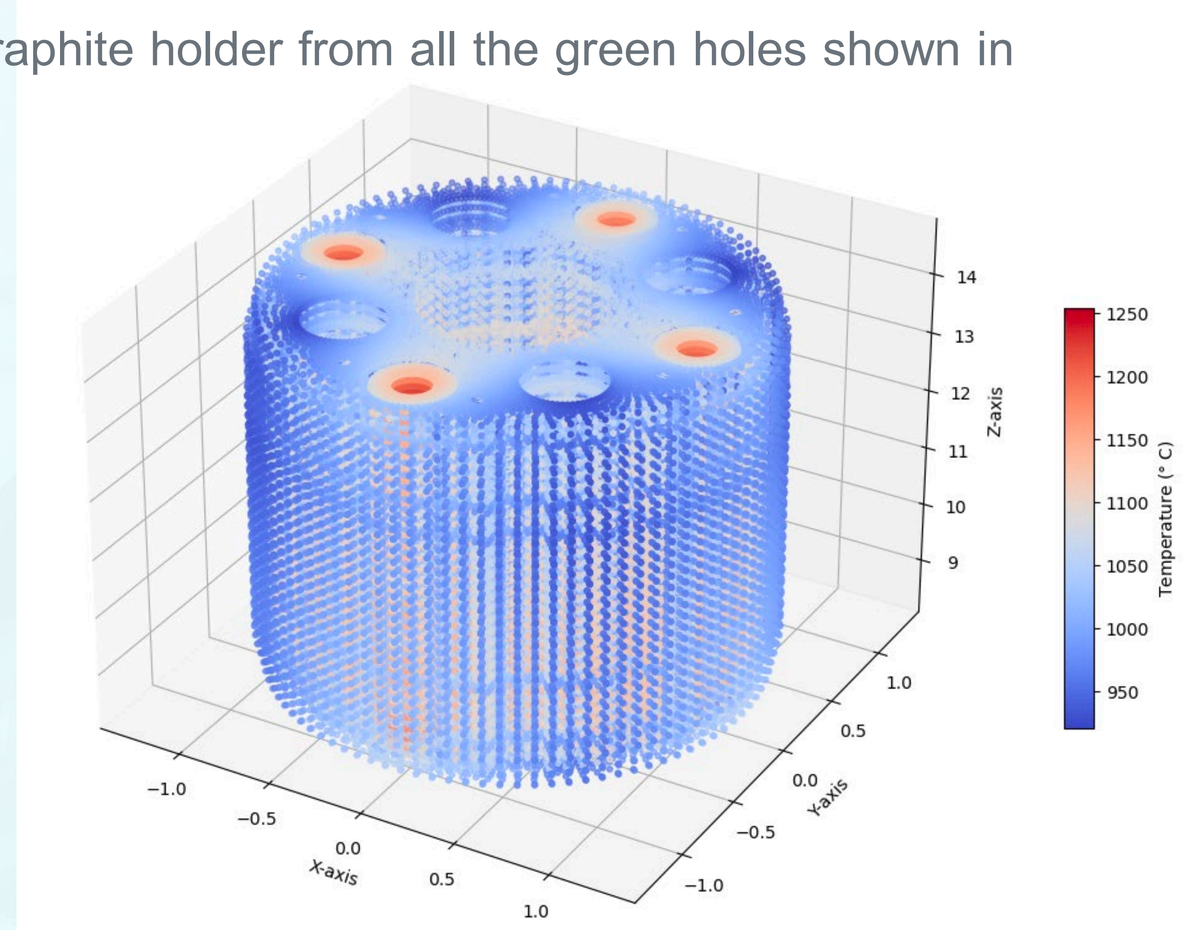

Figure 2 : Graphite Holder 5 with fuel in 3D.

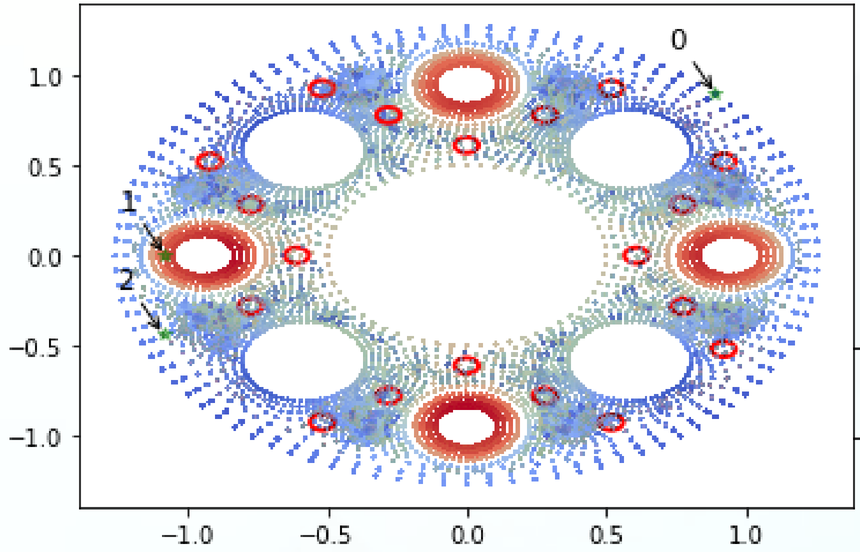

Unconstrained

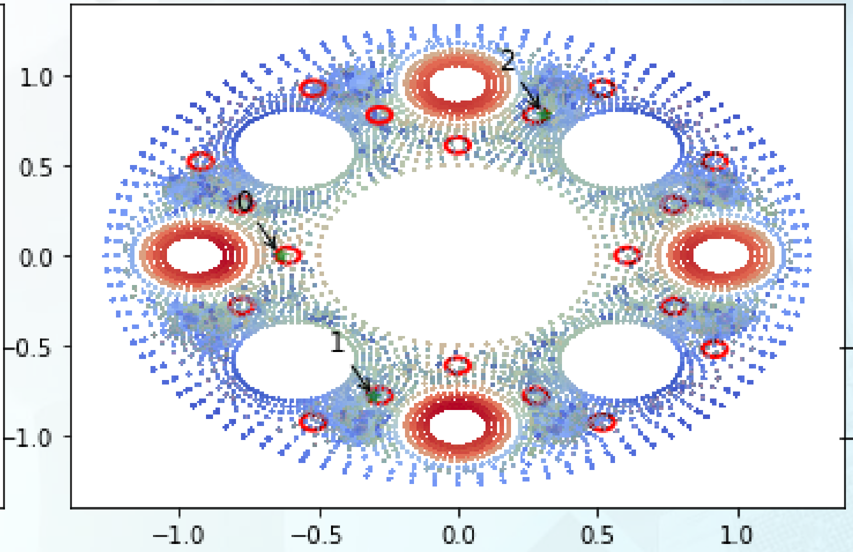

Constrained

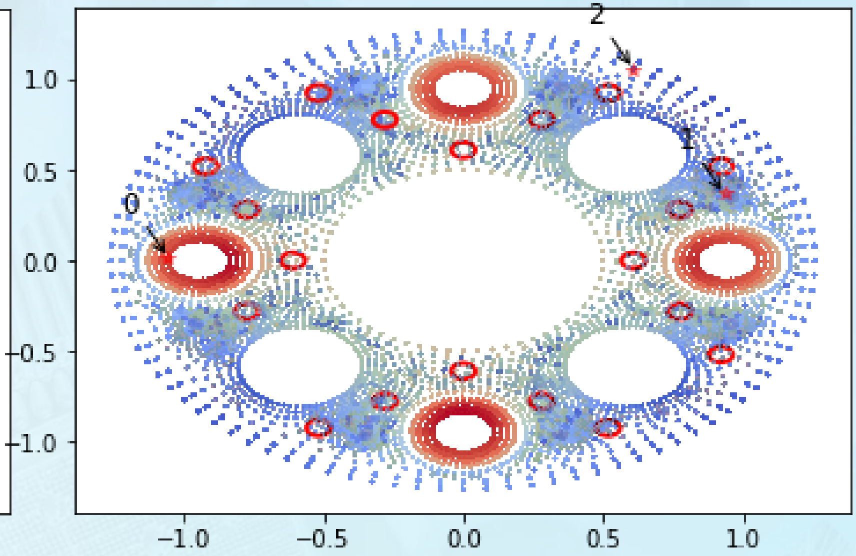

Random

Sensor	X	Y	Z	Sensor	X	Y	Z	Sensor	X	Y	Z
0	0.892	0.892	12.3080	0	-0.638	0.005	9.000	0	-1.050	0.110	11.346
1	-1.081	0.000	14.1535	1	-0.302	-0.781	11.154	1	0.857	0.252	14.000
2	-1.088	-0.438	9.8000	2	0.306	0.783	14.167	2	+0.615	0.892	10.962

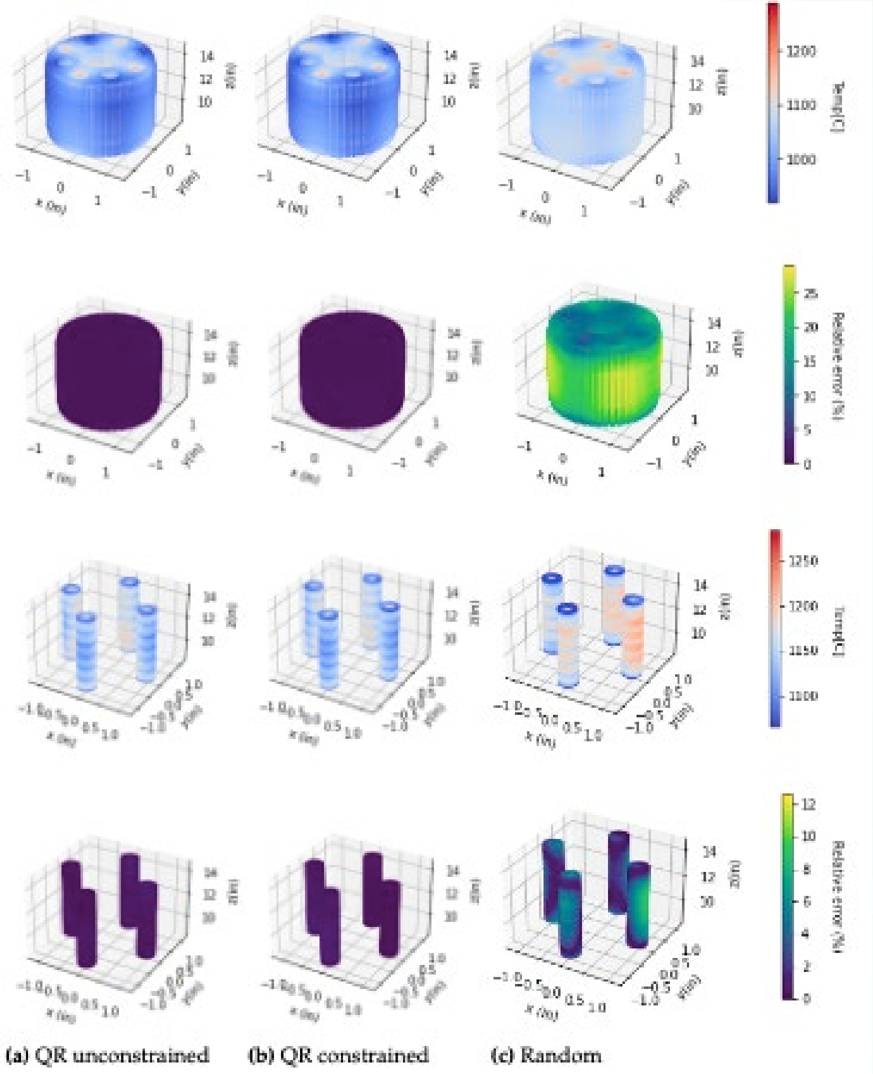

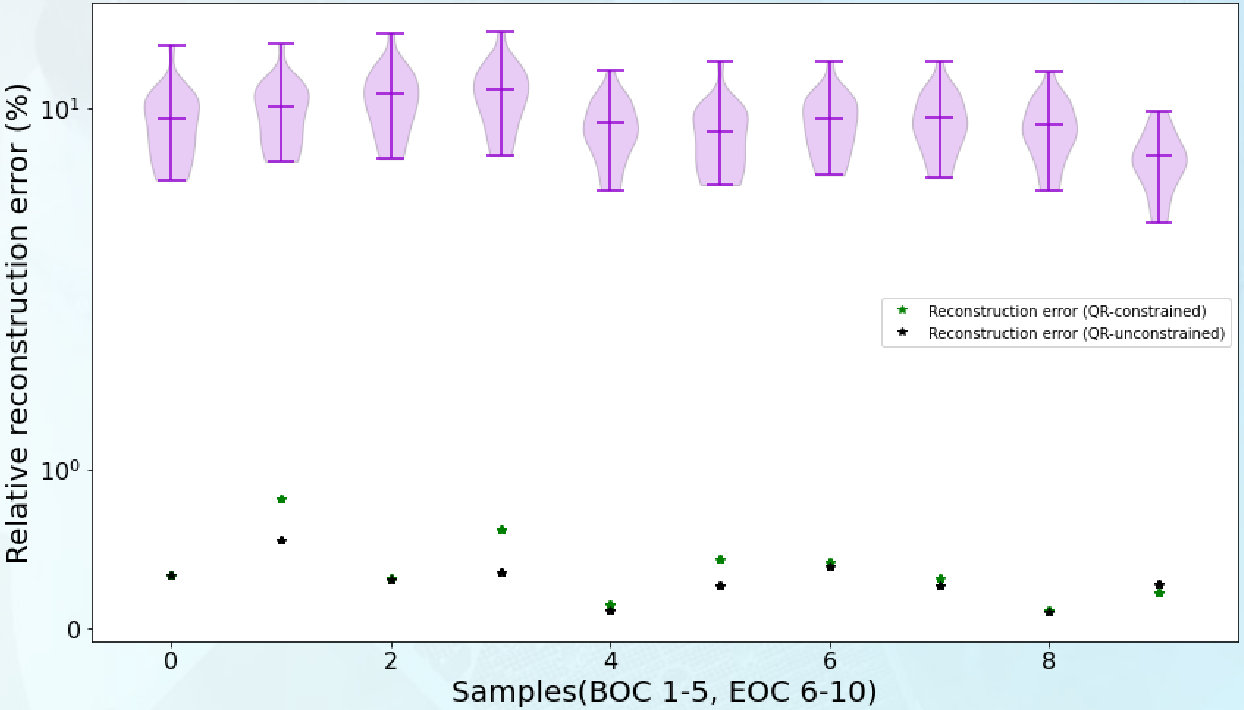

(a-c) Temperature profile reconstructions (d-e) Relative reconstruction errors. Unconstrained optimization leads to a maximum reconstruction error of ε = 0.75% (a,d), while introduction constraints results in ε = 1% (b,e). Random sensor placement (c,f) results in inaccurate reconstructions ε = 25% compared to that of optimized sensor locations

Results - Case Study 3: Steam generator Design

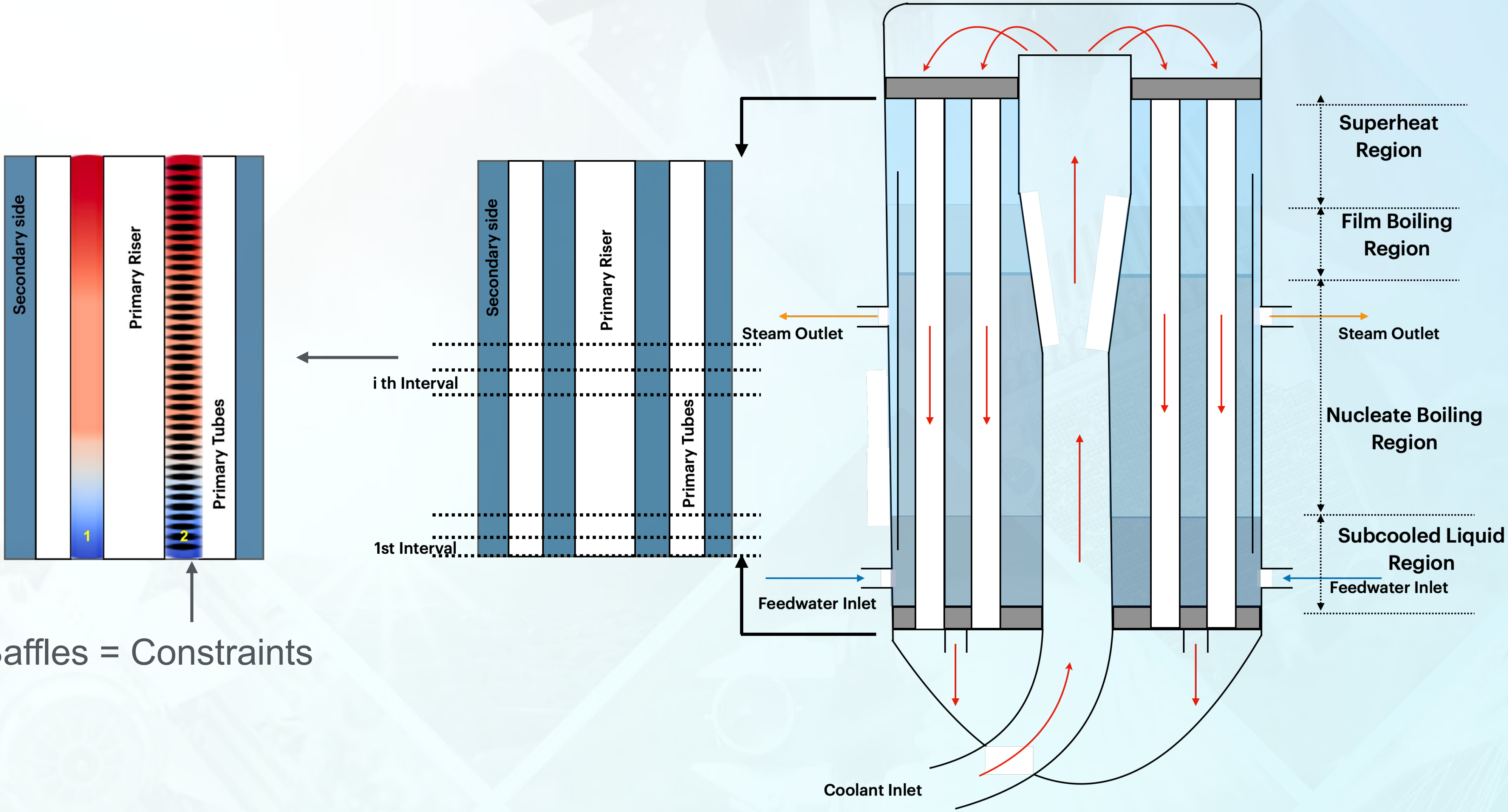

Baffles = Constraints

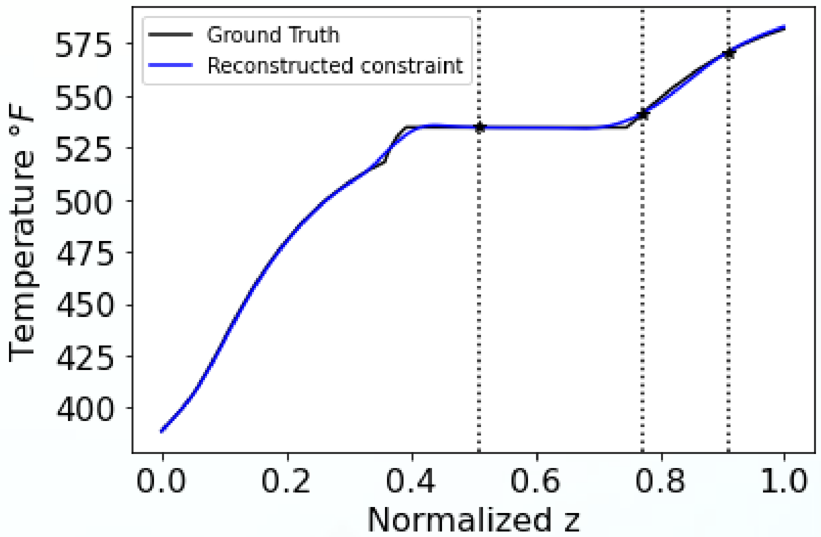

a) Constrained sensor reconstruction ε = 0.9%

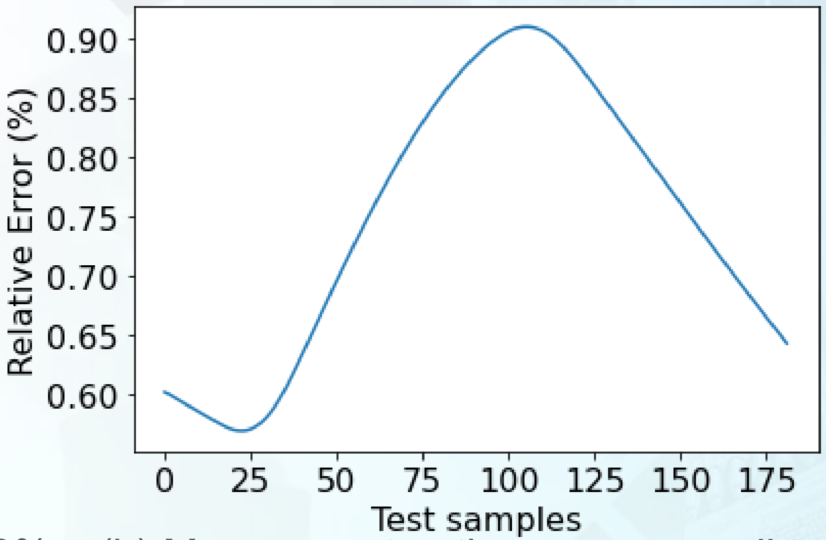

(b) Max reconstruction error over all test samples is 0.9%

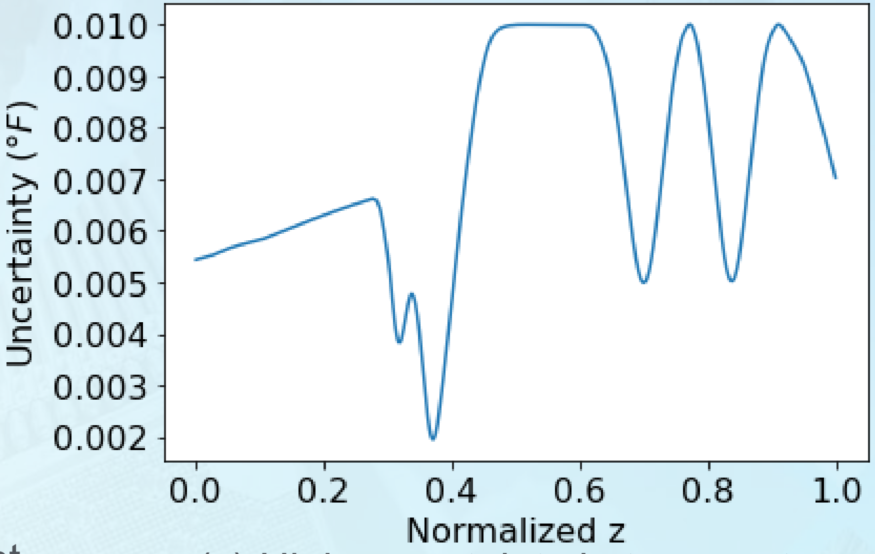

(c) High uncertainty in temperature transition zones

Secondary side temperature profile reconstructed from 3 constrained sensors results in a maximum reconstruction error of 0.9 % over all test samples (a,b) and the maximum uncertainty in reconstruction for noisy sensor measurements is 0.01 °F (c).

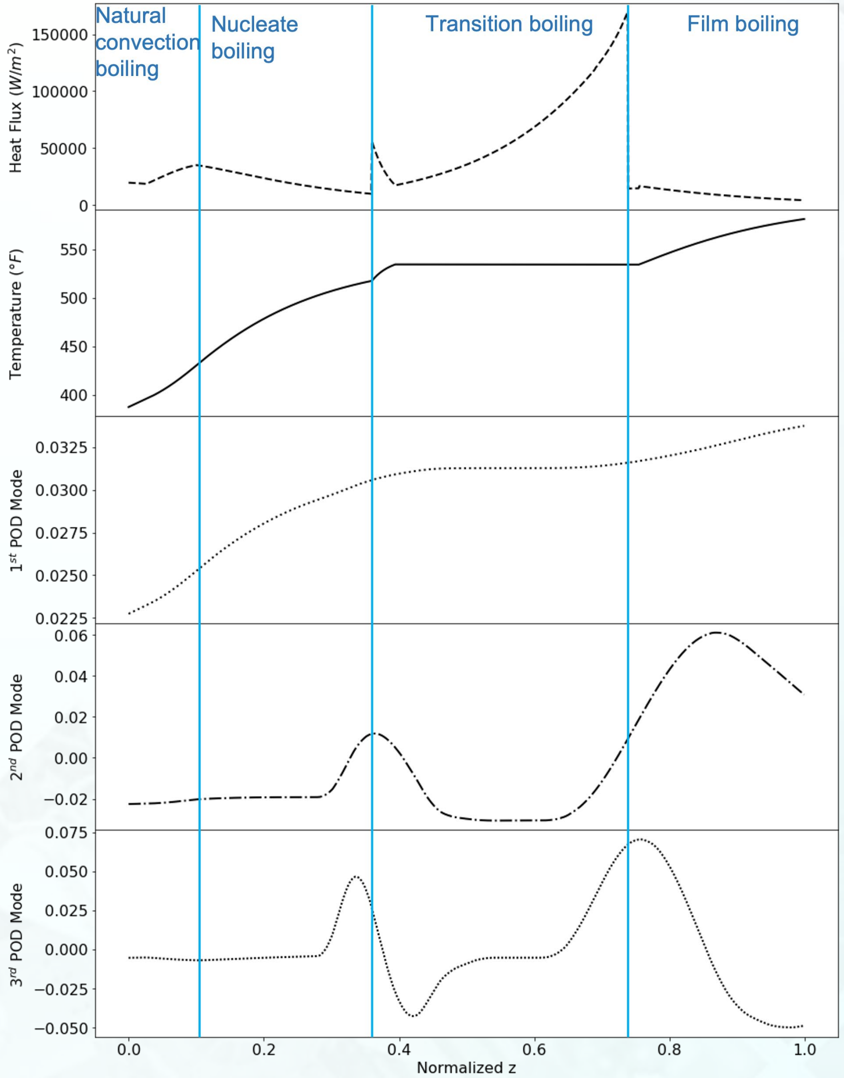

The leading three POD modes of secondary side temperature capture 99 % of energy content and provide accurate reconstructions of temperature fields. The first POD mode captures the secondary side temperature profile whereas the 3rd POD mode captures variation in the heat flux that cause changes in temperature along the normalized z coordinates in the steam generator

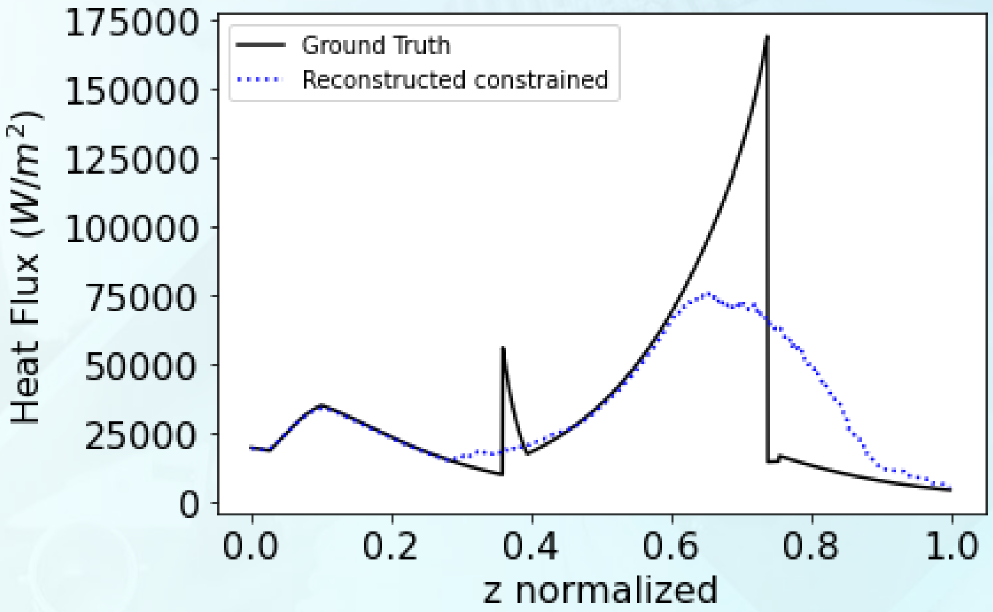

Heat Flux inferred from reconstructed temperature measurements

Concluding Remarks

- Full Field Reconstruction from Optimally Placed X Sparse Sensors **Outperforms** 4X random sensors by **Several Orders of magnitudes** of accuracy.
- Future work includes extending the sensor placement to **anomaly** and **off-normal** conditions **detection**.
- Intellectual property/copy rights: RAVEN Sparse Sensing Postprocessor https://github.com/idaholab/raven/blob/devel/ravenframework/Models/PostProcessors/SparseSensing.py

IEEE Sensors Council IEEE SENSORS JOURNAL, VOL. 24, NO. 9, 1 MAY 2024 15501

Constrained Optimization of Sensor Placement for Nuclear Digital Twins

Niharika Karnik, Mohammad G. Abdo, Carlos E. Estrada-Perez, Jun Soo Yoo, Joshua J. Cogliati, Richard S. Skifton, Pattrick Calderoni, Steven L. Brunton, *Senior Member, IEEE*, and Krithika Manohar, *Member, IEEE*

Abstract—The deployment of extensive sensor arrays in nuclear reactors is infeasible due to challenging operating conditions and inherent spatial limitations. Strategically placing sensors within defined spatial constraints is essential for the reconstruction of reactor flow fields and the creation of nuclear digital twins. We develop a data-driven technique that incorporates constraints into an optimization framework for sensor placement, with the primary objective of minimizing reconstruction errors under noisy sensor measurements. The proposed greedy algorithm optimizes sensor locations over high-dimensional grids, adhering to user-specified constraints. We demonstrate the efficacy of optimized sensors by exhaustively computing all feasible configurations for a low-dimensional dynamical system. To validate our methodology, we apply the algorithm to the Out-of-Pile Testing and Instrumentation Transient Water Irradiation System (OPTI-TWIST heated to emulate the neutronic effect of the nuclear fuel. The TWIST Transient Reactor Test Facility (TREAT) at the Idaho National Labor The resulting sensor-based temperature reconstruction within OPTI probabilistic bounds for noise-induced uncertainty, and establishes a twin and the experimental facility.

Index Terms—Digital twins, optimization, reduced-order models, straints.

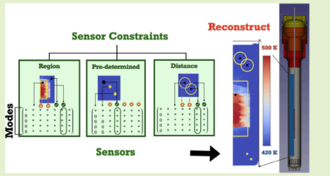

I. Introduction

SAFE and efficient performance of nuclear power plants require remote monitoring, condition-based maintenance, and real-time control via data streamed from physical processes [1], especially in advanced reactors (e.g.,

Manuscript received 16 January 2024; revised 9 February 2024; accepted 10 February 2024. Date of publication 28 February 2024; date of current version 1 May 2024. This work was supported by the INL Laboratory Directed Research and Development (LDRD) Program through the DOE Idaho Operations Office under Contract DE-AC07-05ID14517 for LDRD-22A1059-091FP. The work of Steven L. Brunton and Krithika Manohar was supported by the NSF AI Institute in Dynamic Systems under Grant 2112085. The associate editor coordinating the review of this article and approving it for publication was Dr. Andre E. Lazzaretti. *(Corresponding authors: Niharika Karnik; Mohammad G. Abdo; Krithika Manohar.)*

Niharika Karnik, Steven L. Brunton, and Krithika Manohar are with the Department of Mechanical Engineering, University of Washington, Seattle, WA 98195 USA (e-mail: nkarnik@uw.edu; sbrunton@uw.edu; kmanohar@uw.edu).
Mohammad G. Abdo, Carlos E. Estrada-Perez, Jun Soo Yoo, Joshua J. Cogliati, Richard S. Skifton, and Pattrick Calderoni are with Idaho National Laboratory, Idaho Falls, ID 83415 USA (e-mail: Mohammad.Abdo@inl.gov; Carlos.EstradaPerez@inl.gov; JunSoo.Yoo@inl.gov; joshua.cogliati@inl.gov; richard.skifton@inl.gov; pattrick.calderoni@inl.gov).
Digital Object Identifier 10.1109/JSEN.2024.3368875

energies MDPI

Article

Leveraging Optimal Sparse Sensor Placement to Aggregate a Network of Digital Twins for Nuclear Subsystems

Niharika Karnik [1,*], Congjian Wang [2], Palash K. Bhowmik [2], Joshua J. Cogliati [2], Silvino A. Balderrama Prieto [2], Changhu Xing [2], Andrei A. Klishin [1], Richard Skifton [2], Musa Moussaoui [2], Charles P. Folsom [2], Joe J. Palmer [2], Piyush Sabharwall [2], Krithika Manohar [1,*] and Mohammad G. Abdo [2,*]

1 Department of Mechanical Engineering, University of Washington, Seattle, WA 98195, USA; aklishin@uw.edu
2 Idaho National Laboratory, Idaho Falls, ID 83415, USA; congjian.wang@inl.gov (C.W.); palashkumar.bhowmik@inl.gov (P.K.B.); joshua.cogliati@inl.gov (J.J.C.); silvino.balderramaprieto@inl.gov (S.A.B.P.); changhu.xing@inl.gov (C.X.); richard.skifton@inl.gov (R.S.); musa.moussaoui@inl.gov (M.M.); charles.folsom@inl.gov (C.P.F.); joe.palmer@inl.gov (J.J.P.); piyush.sabharwall@inl.gov (P.S.)
* Correspondence: nkarnik@uw.edu (N.K.); kmanohar@uw.edu (K.M.); mohammad.abdo@inl.gov (M.G.A.)

Abstract: Nuclear power plants (NPPs) require continuous monitoring of various systems, structures, and components to ensure safe and efficient operations. The critical safety testing of new fuel compositions and the analysis of the effects of power transients on core temperatures can be achieved through modeling and simulations. They capture the dynamics of the physical phenomenon associated with failure modes and facilitate the creation of digital twins (DTs). Accurate reconstruction

References

- Krithika Manohar, J Nathan Kutz, and Steven L Brunton. “Optimal sensor and actuator selection using balanced model reduction”. In: IEEE Transactions on Automatic Control 67.4 (2021), pp. 2108–2115.
- Karnik, N., **Abdo, M. G.**, Estrada-Perez, C. E., Yoo, J. S., Cogliati, J. J., Skifton, R. S., ... & Manohar, K. (2024). “Constrained optimization of sensor placement for nuclear digital twins.” IEEE Sensors Journal. (published 02/28/2024)
- Karnik, N., **M. G. Abdo**, and K. Manohar. “Optimal Sparse Sensor Placement with Adaptive Constraints for Nuclear Digital Twins." 75th Annual Meeting of the APS Division of Fluid Dynamics (APS DFD 2022) November 20-22, 2022, Indianapolis, IN.
- DICE 2024: presentation about applications of sparse sensing in nuclear digital twins.
- Karnik, N., **Abdo, M. G.**, Manohar K. “Data-Driven Sensor Placement for Nuclear Reactor Transient Analyses in Digital Twins”. Bulletin of the American Physical Society
- AI Institute in Dynamic Systems CTF workshop (Sponsored by NSF)
- PHSOR 2024, Scintific ML workshop: “Sparse sensing and Sparse Learning for Nuclear Digital Twins.”

Concluding Remarks

The traditional mindset looks at M&S after design, prototyping, building, and maybe even experimenting. The paradigm shift is to incorporate modeling and ML in each step a long the pipeline. Nuclear applications lack the luxury of immersive instrumentation. Thus, this instrumentation must be carefully and optimally placed to gain the maximum knowledge/insights from the dynamical process.

Mohammad G. Abdo, Ph.D.

Modeling and Simulation Scientist | Digital Reactor Technology and Development (C160)

Reactor Systems Design and Analysis | NS&T

mohammad.abdo@inl.gov | REC EROB IF-654 3EL103 | Phone: 208-526-4640

Idaho National Laboratory | 2525 Fremont Ave. | Idaho Falls, ID | 83415

ORCiD: 0000-0001-9845-6978

https://www.linkedin.com/in/mohammad-abdo-a7625082/

https://www.researchgate.net/profile/Mohammad-Abdo/research

https://github.com/Jimmy-INL

LinkedIn

ResearchGate

GitHub

Thanks for attention!


INL
Idaho National Laboratory

Backup Slides

Illustration of QR with Column Pivoting

QR factorization: Orthonormal Q, upper-triangular R, permutation $\mathbb{S}$

- $|\det \mathbb{S}\Phi_r|$ = product of (magnitudes of) diagonal entries of R
- Pivot indices correspond to optimal sensor locations
- We enforce constraints by selecting the next pivot from the admissible locations.

Selecting sensors/pivots in the admissible locations

Column with Maximal Two Norm $\|\boldsymbol{\theta}\|_2$ from constrained indices

$$\boldsymbol{\Phi}_r^T \mathbb{S}^T = \begin{array}{c} \begin{array}{ccccccc} & & & & & \boldsymbol{\theta} & \end{array} \\ \left(\begin{array}{cccc|ccc} * & * & * & * & * & * & * \\ * & * & * & * & * & * & * \\ * & * & * & * & * & * & * \\ * & * & * & * & * & * & * \end{array}\right) \end{array} \mathbb{S}^T = \mathrm{QR} = \mathrm{Q} \left(\begin{array}{cccc|ccc} * & * & * & * & * & * & * \\ * & * & * & * & * & * & * \\ * & * & * & * & * & * & * \\ * & * & * & * & * & * & * \end{array}\right)$$

Column's corresponding to constrained sensors

Illustration of QR with Column Pivoting

QR factorization: Orthonormal Q, upper-triangular R, permutation $\mathbb{S}$

- $|\det \mathbb{S}\Phi_r|$ = product of (magnitudes of) diagonal entries of R
- Pivot indices correspond to optimal sensor locations
- We enforce constraints by selecting the next pivot from the admissible locations.

Selecting sensors/pivots in the admissible locations

Update

$$\Phi_r^T \mathbb{S}^T = \left(\begin{array}{cccc|ccc} * & * & * & * & * & * & * \\ * & * & * & * & * & * & * \\ * & * & * & * & * & * & * \\ * & * & * & * & * & * & * \\ * & * & * & * & * & * & * \end{array}\right) \mathbb{S}^T = QR = Q \left(\begin{array}{cccc|ccc} * & * & * & * & * & * & * \\ * & * & * & * & * & * & * \\ * & * & * & * & * & * & * \\ * & * & * & * & * & * & * \end{array}\right)$$

Swap with first

Column corresponding to constrained sensors

Illustration of QR with Column Pivoting

QR factorization: Orthonormal Q, upper-triangular R, permutation $\mathbb{S}$

- $|\det \mathbb{S}\Phi_r|$ = product of (magnitudes of) diagonal entries of R
- Pivot indices correspond to optimal sensor locations
- We enforce constraints by selecting the next pivot from the admissible locations.

Selecting sensors/pivots in the unconstrained locations

Column with Maximal Two Norm $||\theta||_2$ from unconstrained indices

$$\Phi_r^T \mathbb{S}^T = \begin{array}{c} \left(\begin{array}{cccc|ccc} * & * & * & * & * & * & * \\ * & * & * & * & * & * & * \\ * & * & * & * & * & * & * \\ * & * & * & \cancel{*} & * & * & * \end{array}\right) \\ \begin{array}{ccccccc} & & & & \theta & & \end{array} \end{array} \mathbb{S}^T = \mathrm{QR} = \mathrm{Q} \left(\begin{array}{cccc|ccc} * & * & * & * & * & * & * \\ * & * & * & * & * & * & * \\ * & * & * & * & * & * & * \\ * & * & * & * & * & * & * \end{array}\right)$$

Column’s corresponding to constrained sensors

Illustration of QR with Column Pivoting

QR factorization: Orthonormal Q, upper-triangular R, permutation $\mathbb{S}$

- $|\det \mathbb{S}\Phi_r|$ = product of (magnitudes of) diagonal entries of R
- Pivot indices correspond to optimal sensor locations
- We enforce constraints by selecting the next pivot from the admissible locations.

Selecting sensors/pivots in the unconstrained locations

Update

$$\Phi_r^T \mathbb{S}^T = \left(\begin{array}{cccc|ccc} * & * & * & * & * & * & * \\ * & * & * & * & * & * & * \\ * & * & * & * & * & * & * \\ * & * & * & * & * & * & * \end{array}\right) \mathbb{S}^T = QR = Q \left(\begin{array}{cccc|ccc} * & * & * & * & * & * & * \\ * & * & * & * & * & * & * \\ * & * & * & * & * & * & * \\ * & * & * & * & * & * & * \end{array}\right)$$

Swap with second

Column's corresponding to constrained sensors

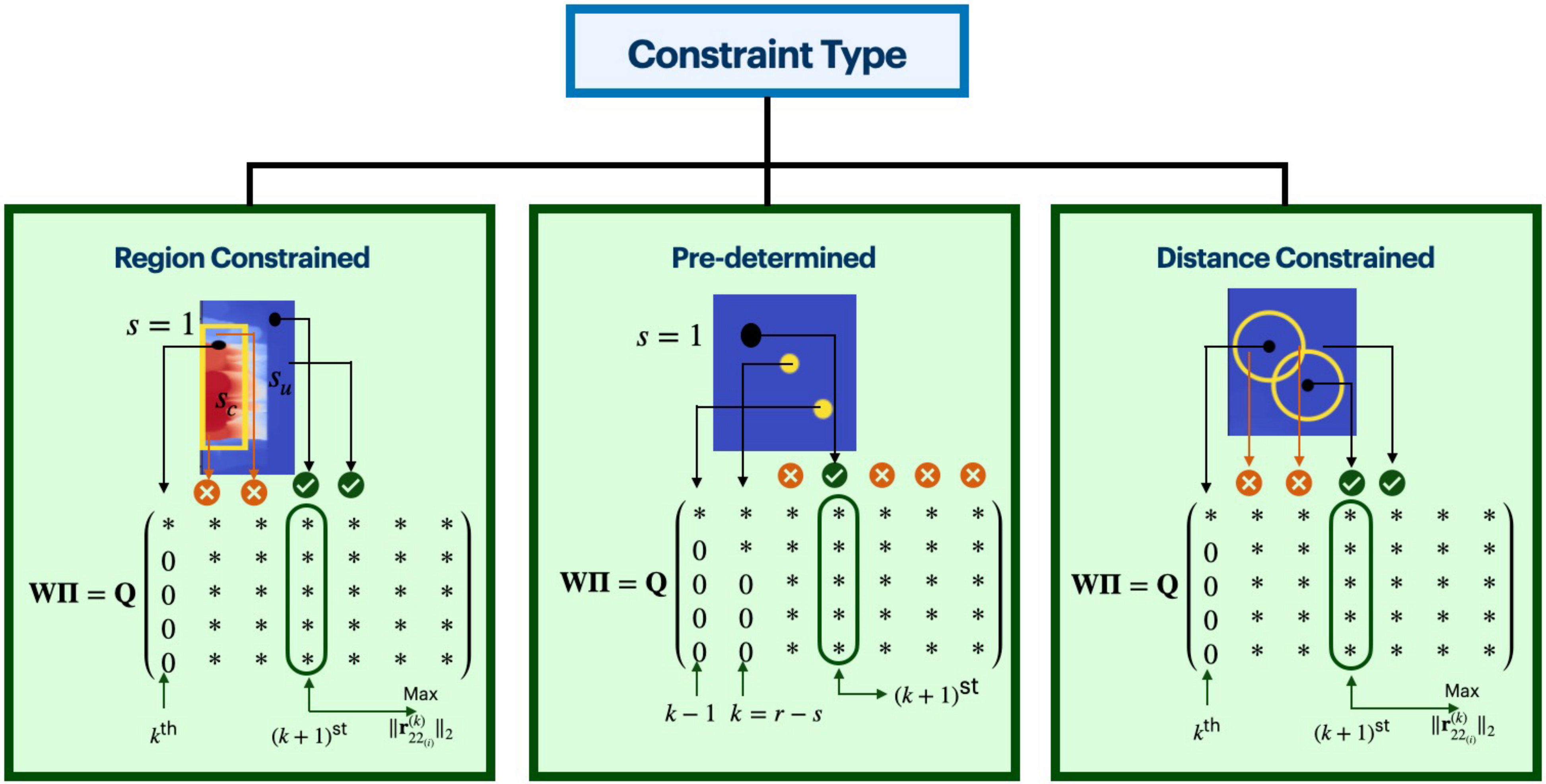
Constraint Type
Region Constrained
Pre-determined
Distance Constrained
s = 1
WΠ = Q
Max
kth
(k + 1)st
k − 1
k = r − s

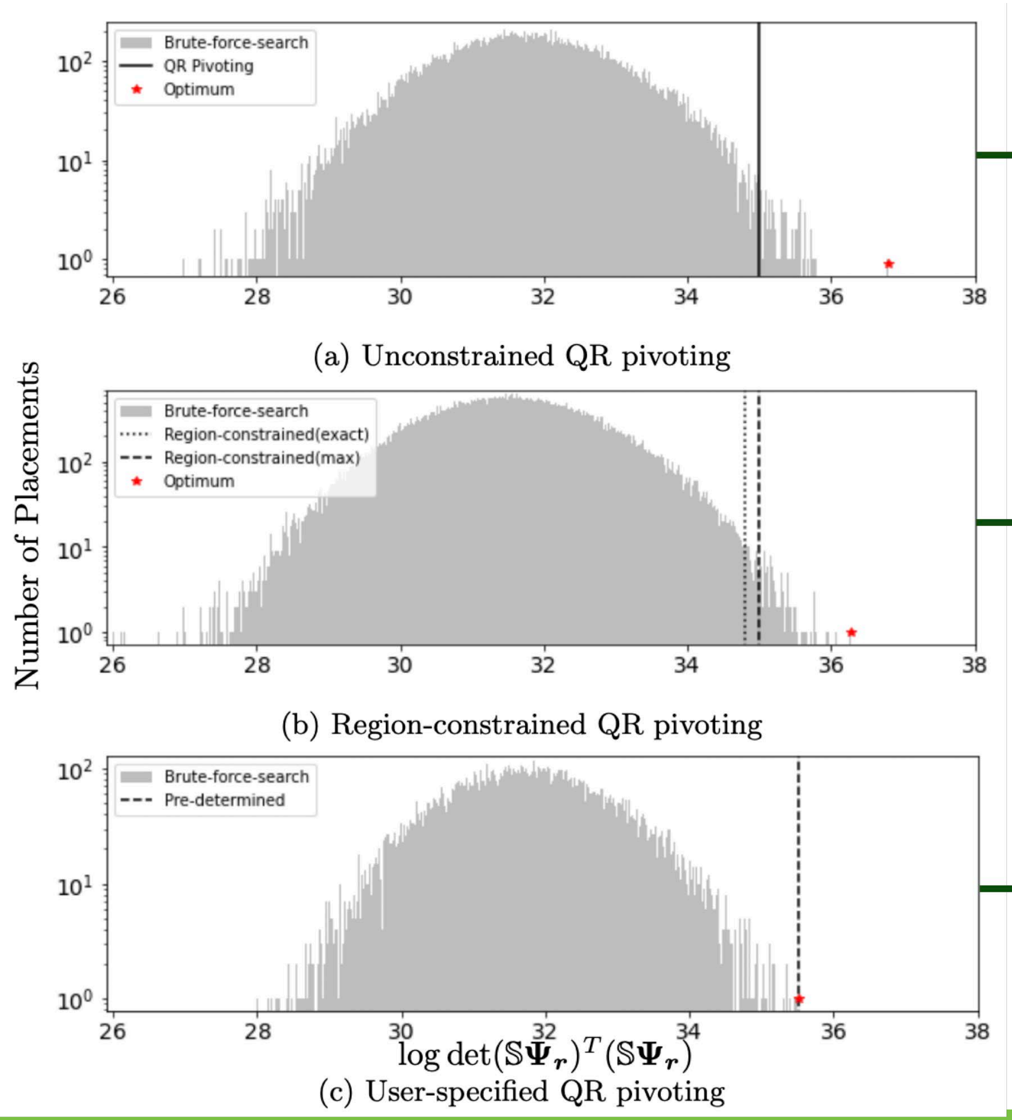

(a) Unconstrained QR pivoting

(b) Region-constrained QR pivoting

(c) User-specified QR pivoting

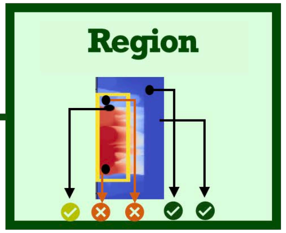

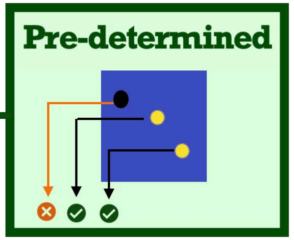

1. Physical Space

(ASI, P&ID, BOM, Actuators)

2. Digital/Virtual Space

(CAD/GUIs/Analytics)

3. Data Space

(Storage, Connectivity, IIoT)

4. Services Space

(Prediction/Monitoring/Control)

In [10]:

```
import Part
CapsuleSTEP = ("/Users/abdomg/projects/Sparse_Sensing_in_NDTs_LDRD/modeling/physics_based/TH_models/CAD/OPTI-TWIST_PerturbPowernBC/TwistCapsule.step")
Capsule = Part.Shape()
Capsule.read(CapsuleSTEP)
Part.show(Capsule)
CapsuleDoc = FreeCAD.ActiveDocument
```

executed in 99ms, finished 17:46:36 2022-06-18

In [11]:

```
render_document(CapsuleDoc)
```

executed in 4.76s, finished 17:46:41 2022-06-18

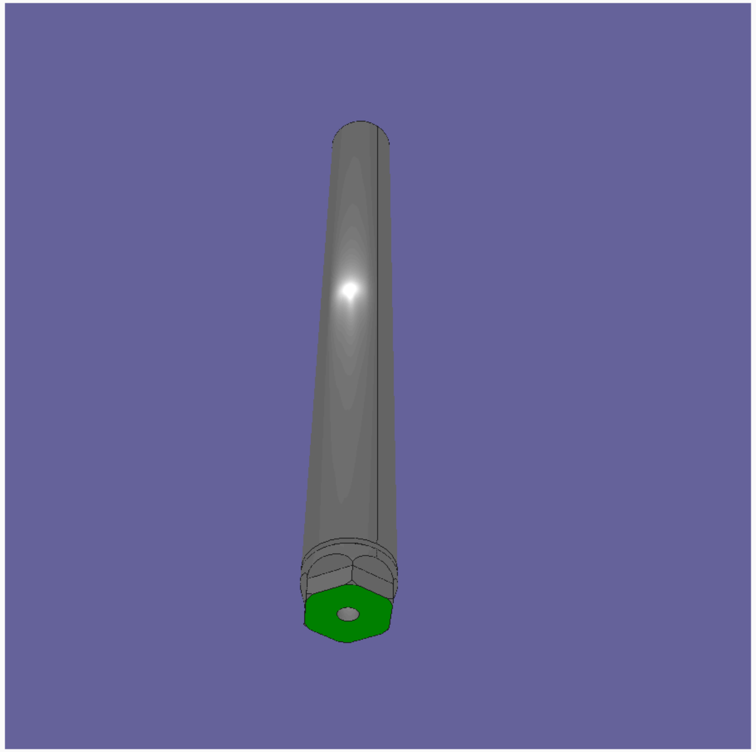

Face19

1. Physical Space

(ASI, P&ID, BOM, Actuators)

2. Digital/Virtual Space

(CAD/GUIs/Analytics)

3. Data Space

(Storage, Connectivity, IIoT)

4. Services Space

(Prediction/Monitoring/Control)

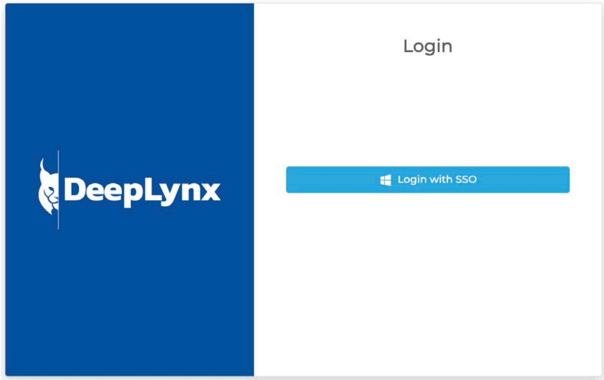

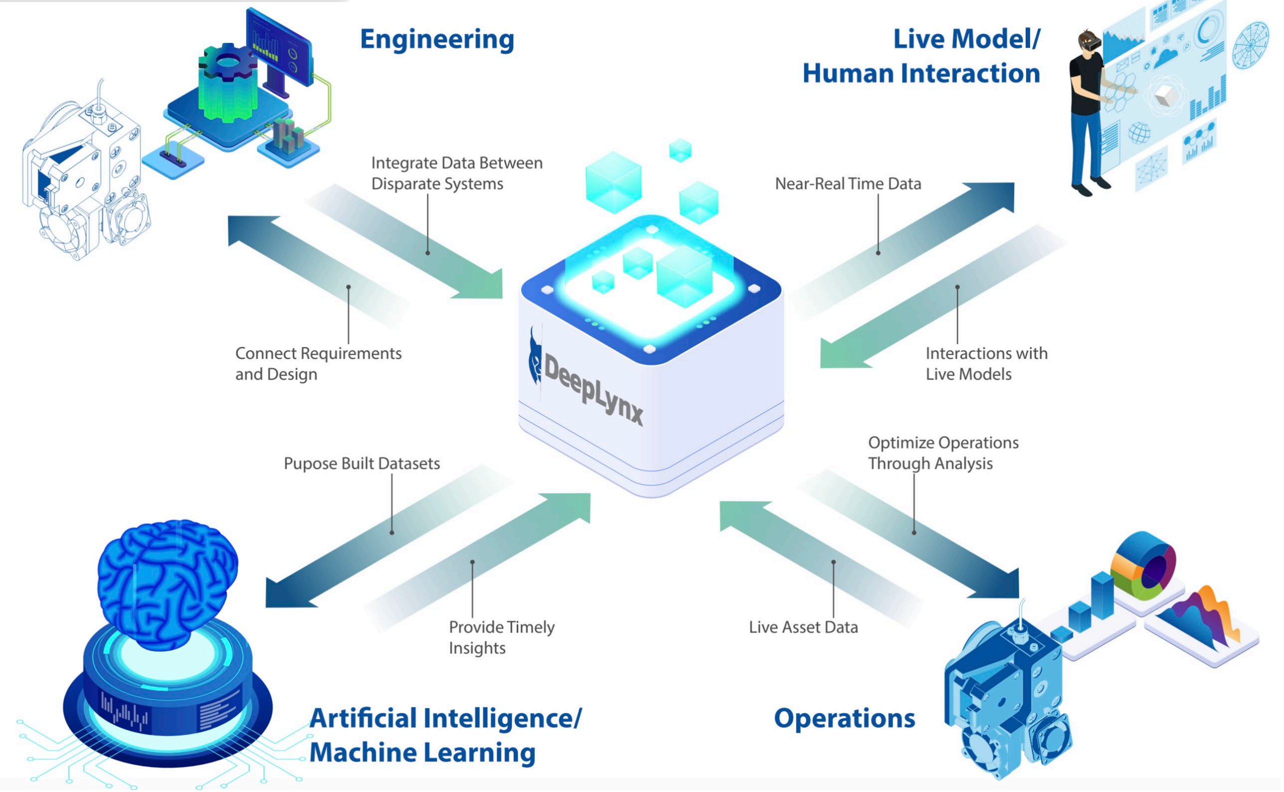

1. Physical Space

(ASI, P&ID, BOM, Actuators)

2. Digital/Virtual Space

(CAD/GUIs/Analytics)

3. Data Space

(Storage, Connectivity, IIoT)

4. Services Space

(Prediction/Monitoring/Control)

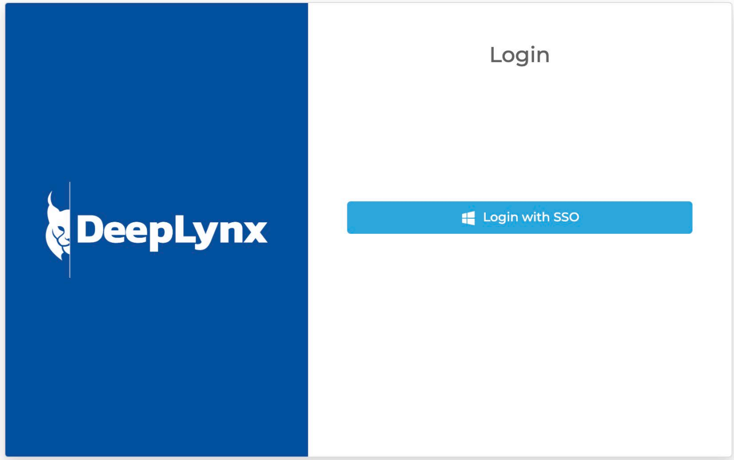

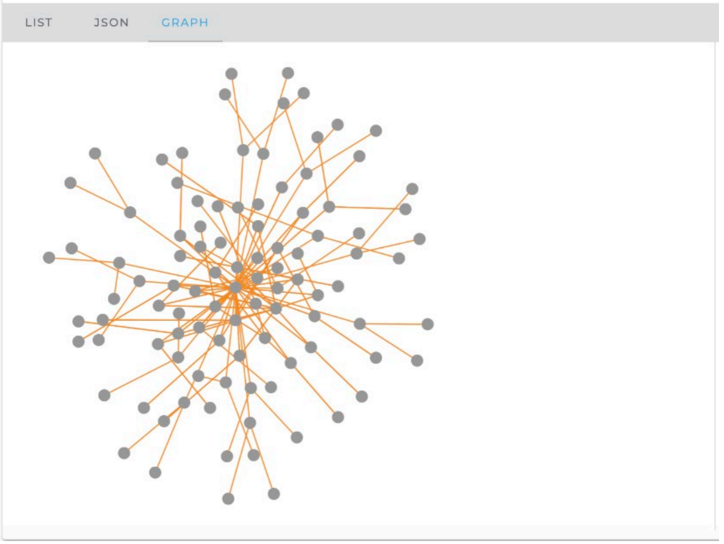

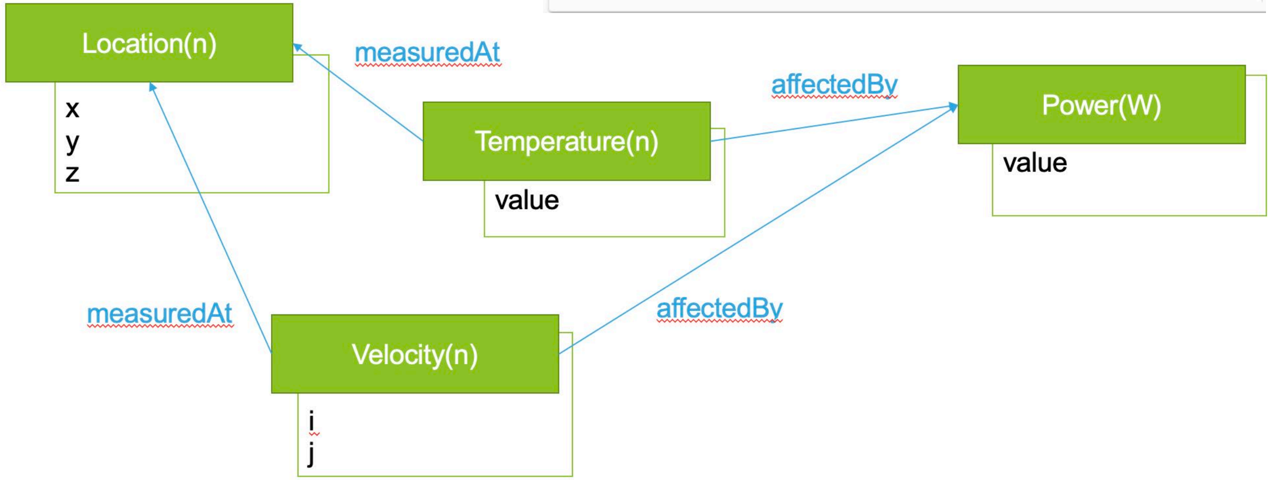

A. 2D Heat Flow through a thin plate

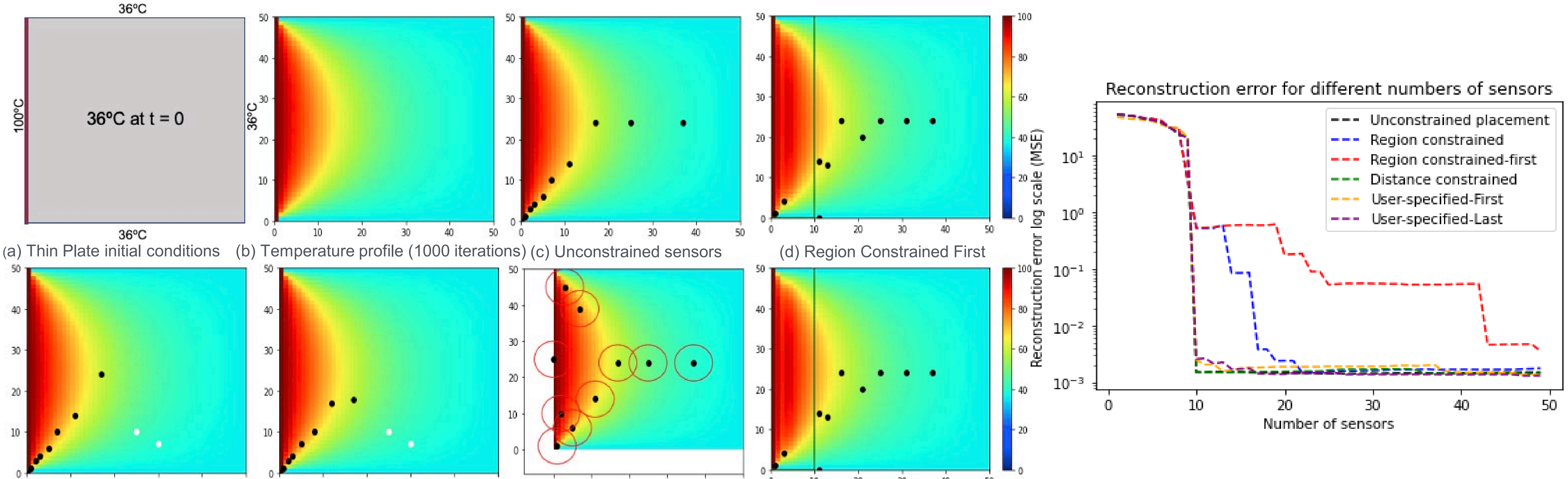

(a) Thin Plate initial conditions (b) Temperature profile (1000 iterations) (c) Unconstrained sensors (d) Region Constrained First

(e) User-specified First (f) User-specified Last (g) Distance Constrained (h) Region Constrained (i) Reconstruction errors for different number of sensors for spatial constraints

Sensor placement for reconstruction of temperature profile of a 2D heat flow through a thin plate for various constrained scenarios.

B. Olivetti faces

unconstrained

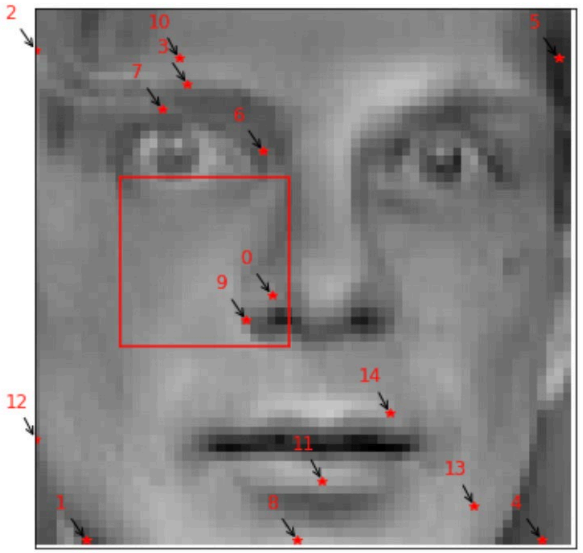

Constrained (exactly 3)

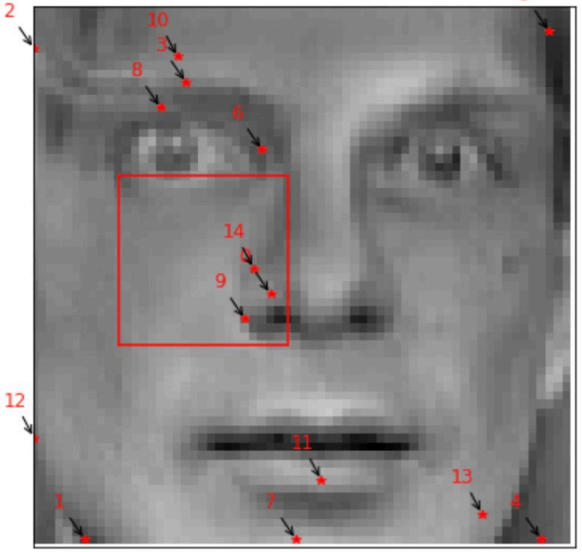

Constrained (max 3)

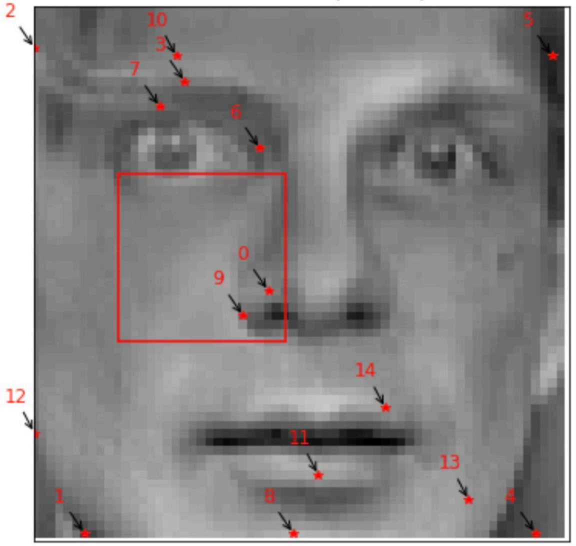

Constrained (max 1)

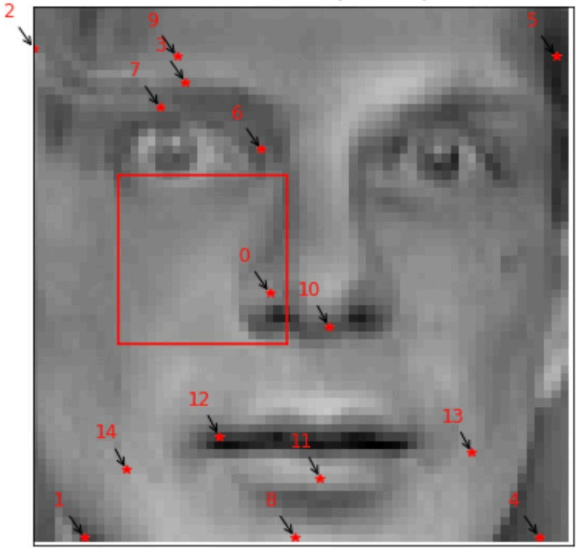

B. Olivetti faces (multiple constrained regions)

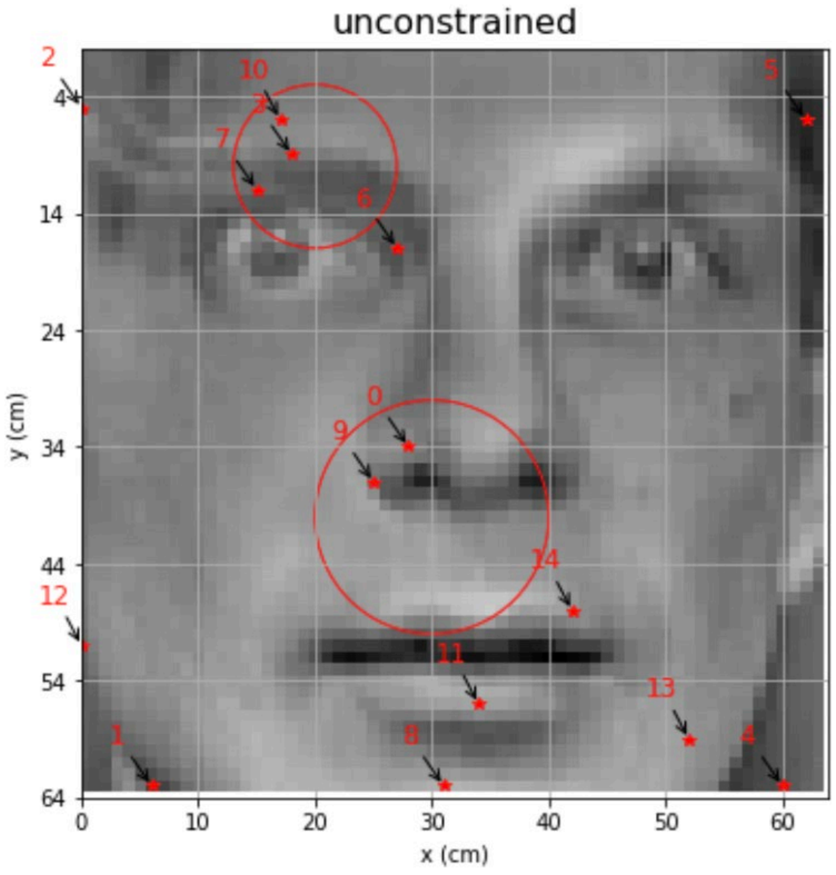

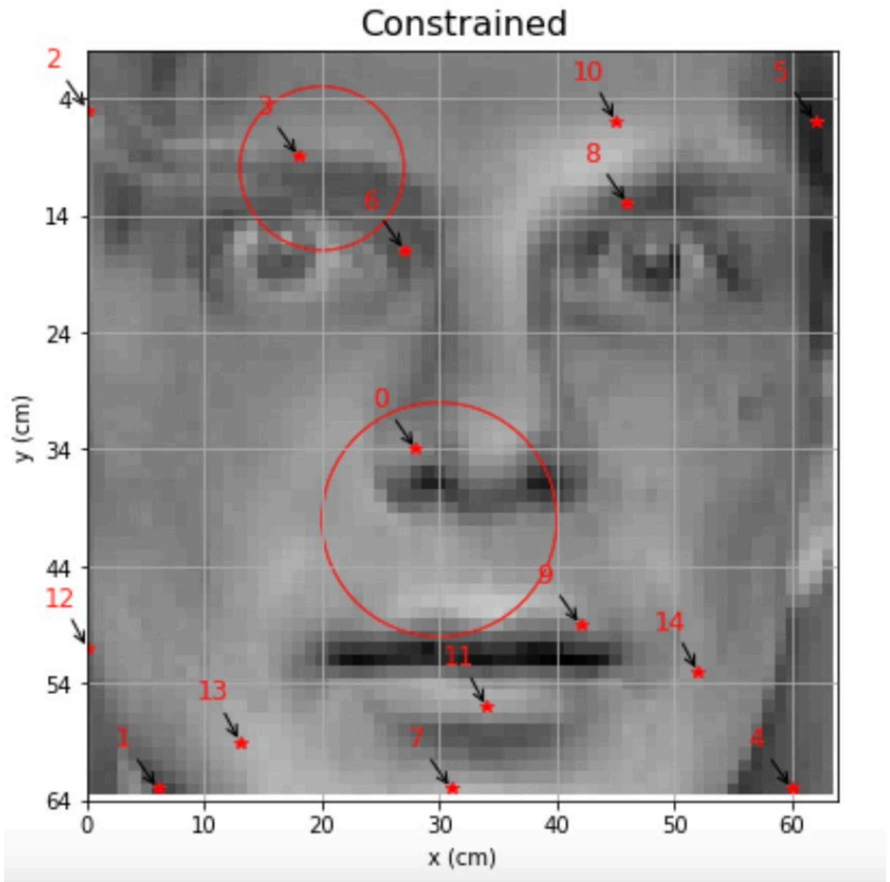

Adding Constraints

- Enable sparse sensing and sparse learning in nuclear digital twins through reconstruction of reactor core flow fields, using optimal sensor placement with spatial constraints such as:
  - User-specified sensor locations
  - Maximum allowable number of sensors restricted regions of a reactor
  - Implicit constraints (not only involving search parameters i.e, grid locations, but also responses of interest i.e., temperature)
  - Sensors located a specific distance apart from each other
  - Using line sensors.
  - Constraining one degree of freedom (holes already bored but at which height should we place the Thermocouple)
- The sparse sensing algorithm is demonstrated on the Opti-TWIST prototype

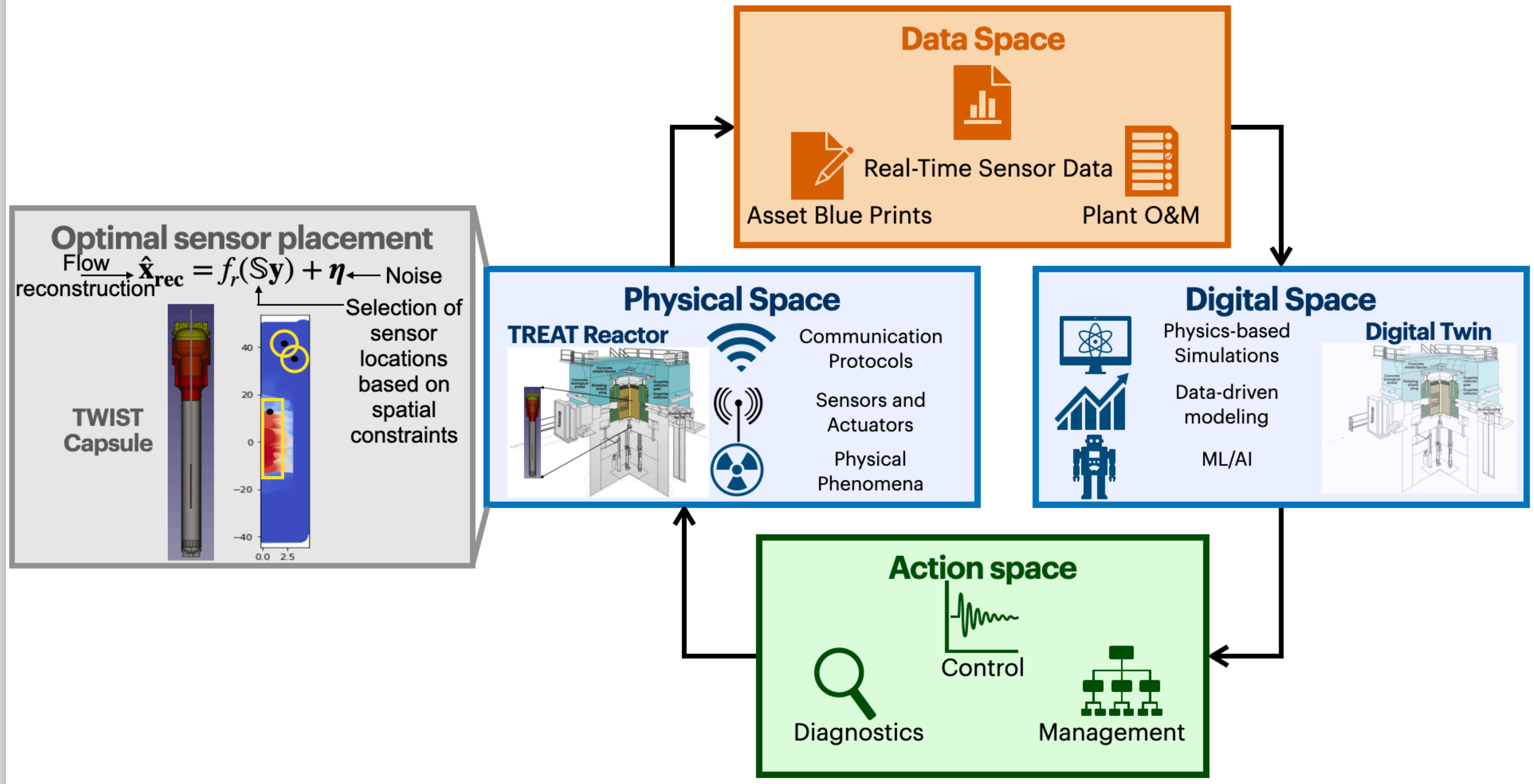

Optimal sensor placement
Flow reconstruction
$\hat{\mathbf{x}}_{\mathbf{rec}} = f_r(\mathbb{S}\mathbf{y}) + \boldsymbol{\eta}$
Noise
Selection of sensor locations based on spatial constraints
TWIST Capsule
Data Space
Real-Time Sensor Data
Asset Blue Prints
Plant O&M
Physical Space
TREAT Reactor
Communication Protocols
Sensors and Actuators
Physical Phenomena
Digital Space
Physics-based Simulations
Data-driven modeling
ML/AI
Digital Twin
Action space
Control
Diagnostics
Management

1. Physical Space

(ASI, P&ID, BOM, Actuators)

2. Digital/Virtual Space

(CAD/GUIs/Analytics)

3. Data Space

(Storage, Connectivity, IIoT)

4. Services Space

(Prediction/Monitoring/Control)

DeepLynx

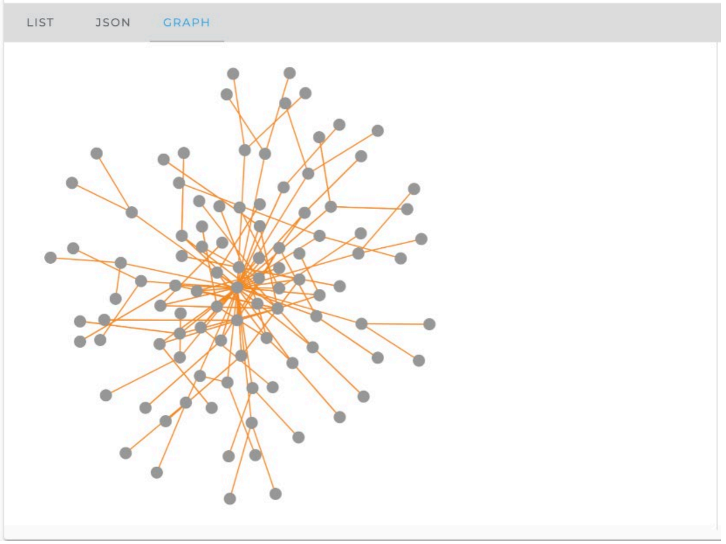

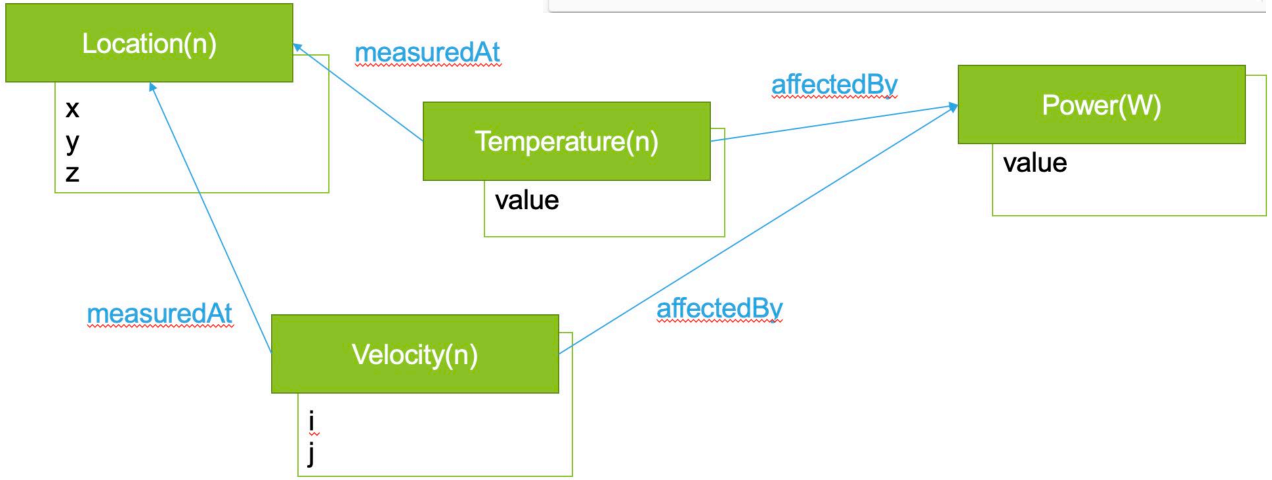

3D CFD Model of the steam generator

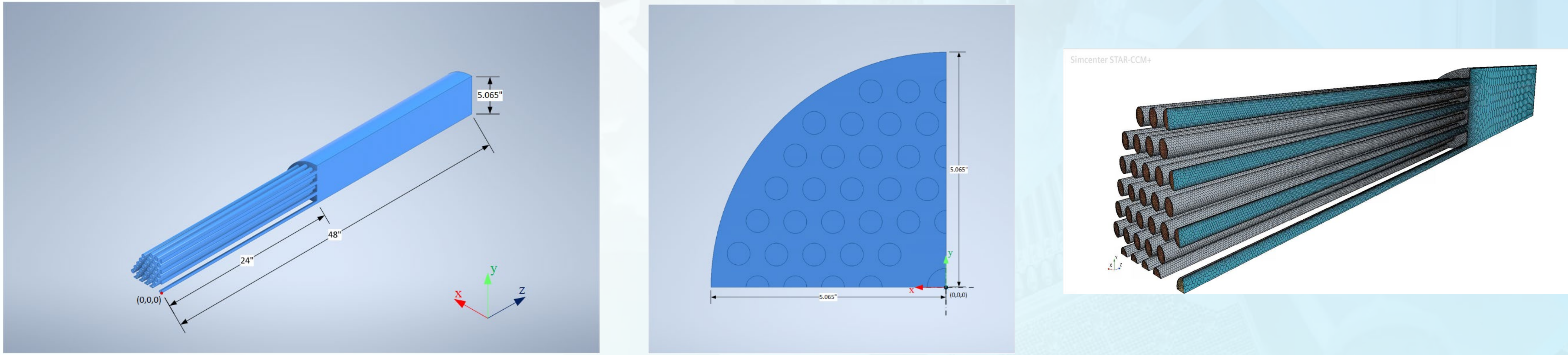

Figure 1. 3D CAD of 1/4th of the SG primary side fluid domain.

	Riser	Upper Shell	SG Tubes
Quantity	1	1	107
ID (in/m)	0.8150/0.0207	10.126/0.2572	0.495/0.0126
OD (in/m)	1.315/0.0334	-	0.625/0.0159
Length (in/m)	451.3/11.46	24/0.6096	24/0.6096
Flow area (in^2/m^2)	0.5217/3.3657x10-4	80.5315/0.0520	0.1924/1.2416x10-4

Table 1. Dimensions of the fluid domain used for CFD analysis.

- Preliminary results are based on assumption of isothermal conditions.
- Total number of grid points = 1882411
- Coarse mesh for the upper shell and fine mesh for the tubes.
- <u>**Sensors can be placed only in the upper shell (beyond 0.6196 m)**</u>
- Calculation of reconstruction error (relative)

$$\frac{|trueValue(sim) \; - sensorReconstructedValue \;|}{trueValue(sim)} \times 100$$

- Calculation of reconstruction error (absolute)

$$|trueValue \; - sensorReconstructedValue|$$

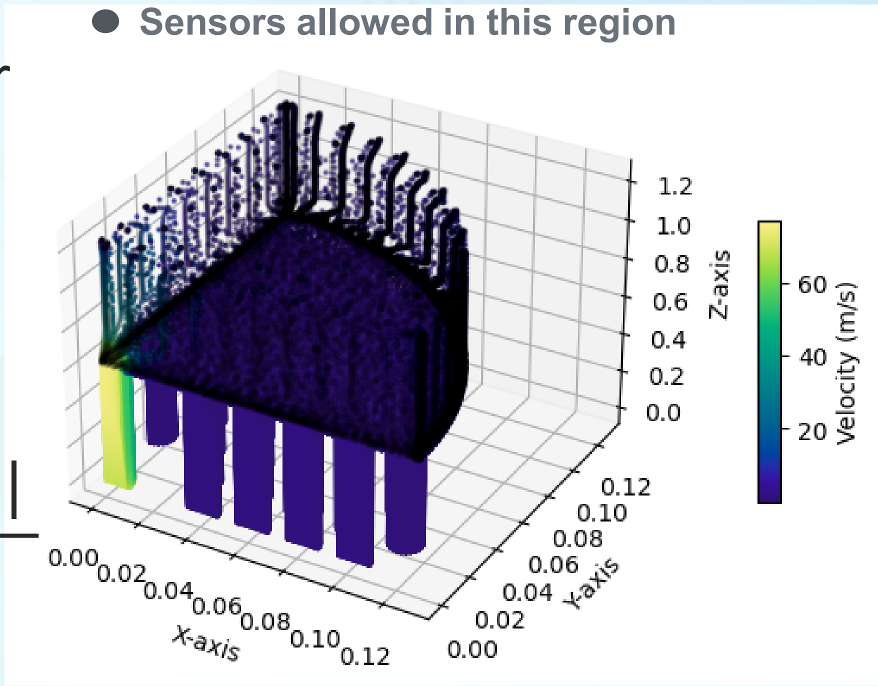

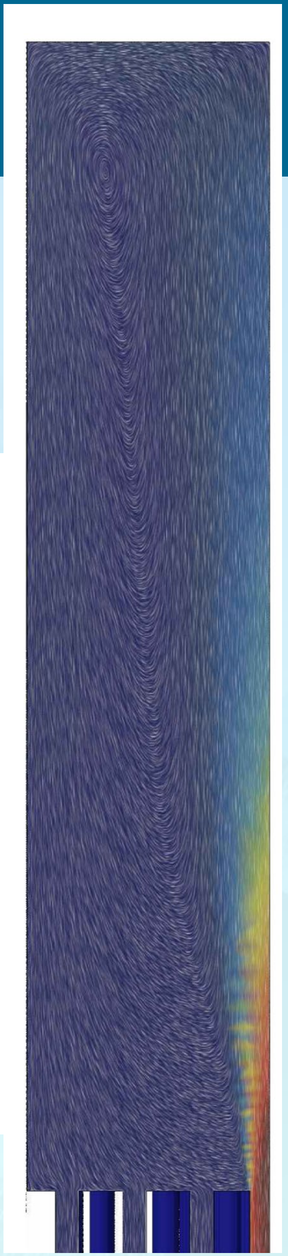

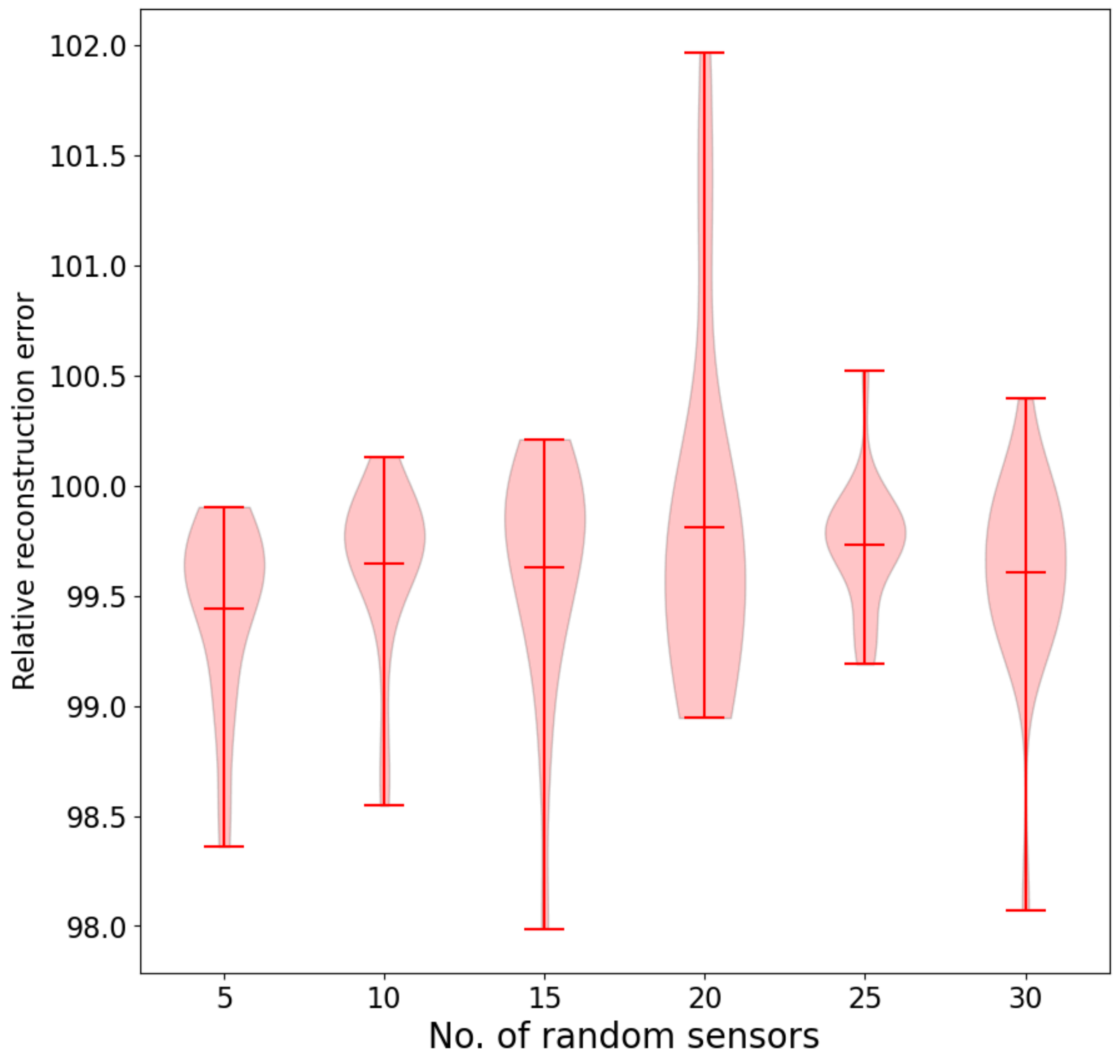

Constrained $error_{rec}$

Random $error_{rec}$

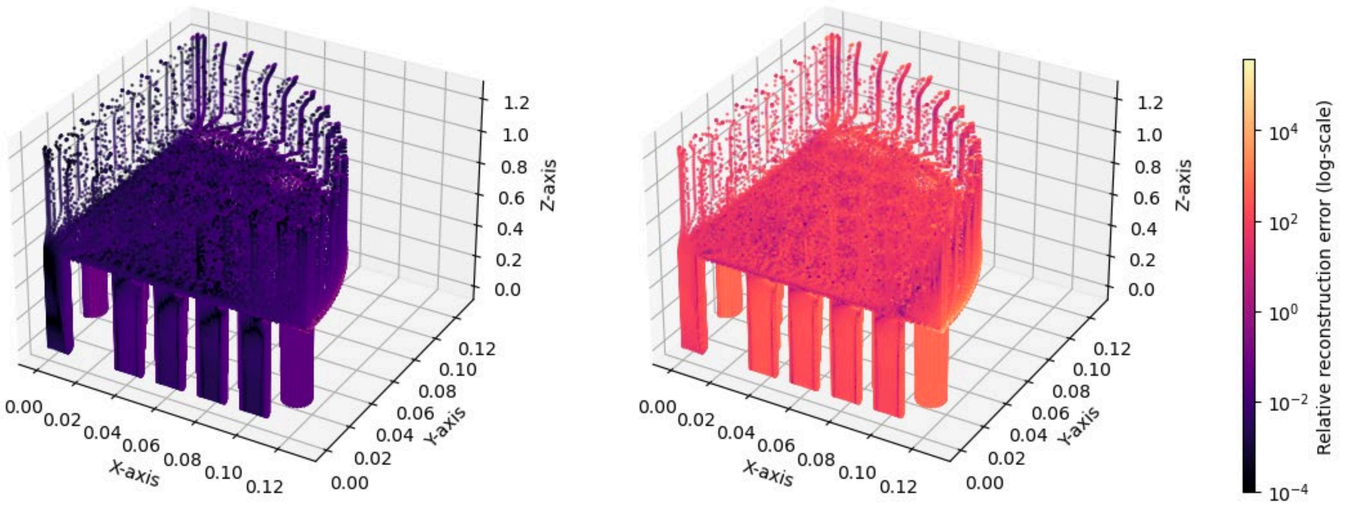

- Preliminary results show a higher average accuracy (~$\mathcal{O}(10^{-1})$) as compared to randomly/intuitively (~$\mathcal{O}(10^{4})$) placing sensors.
- Visualize **vorticity** and **log vorticity** fields for a better idea of the dynamics of the flow and sensor locations.
- Use non-isothermal data for velocity/ log velocity sensor placement and deciding which tubes should carry temperature instrumentation.

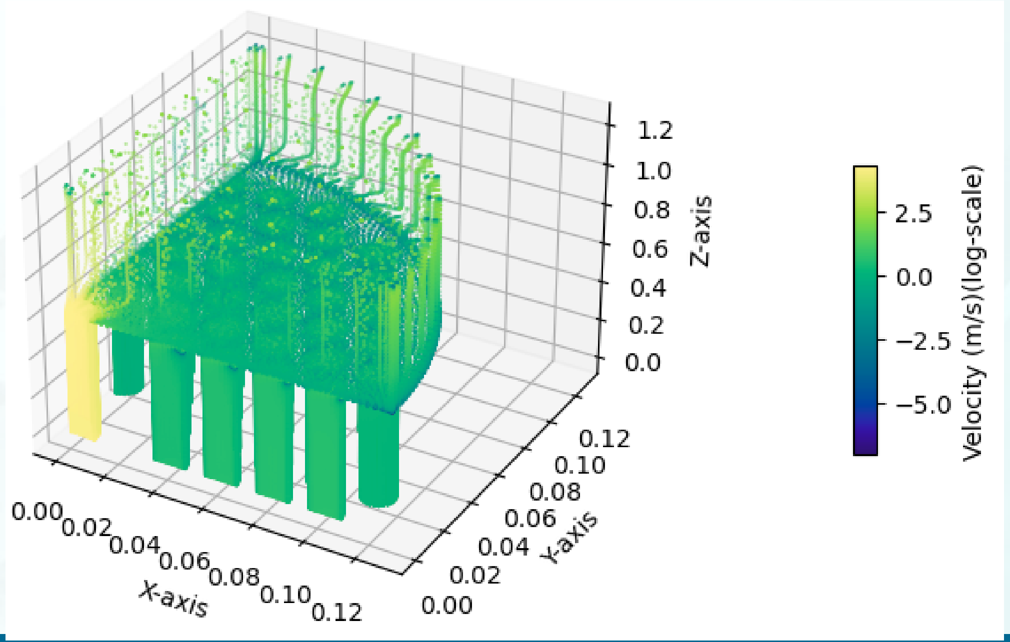

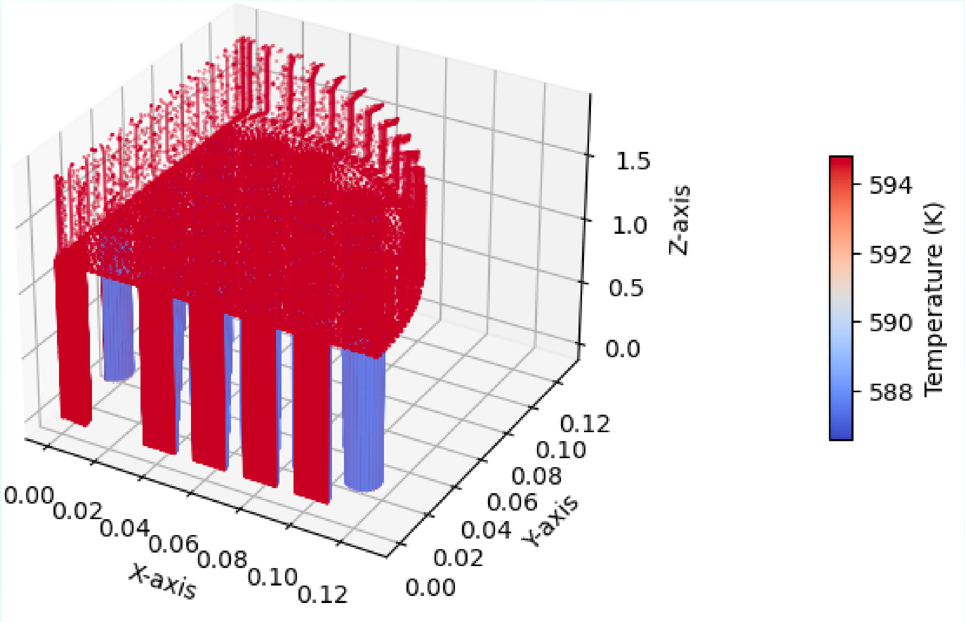

Future Work

- Optimal sensor placement for multi-class classification, (predicting which accident scenario (Loss of Coolant Accident (LOCA), loss of power, etc.)
- Using Mutual Information and Entropy-based metrics for sensor placement.
- Comparing sensor selection to other feature selection algorithms and utilize them to improve selection of sensors.
- Measuring a certain field of interest (e.g., temperature) and inferring another field of interest (e.g., velocity).
- Anomaly detection
- Tensor decomposition instead of Singular value decomposition (SVD) when we have time and samples.
- Implementing constrained sensor placement in RAVEN.

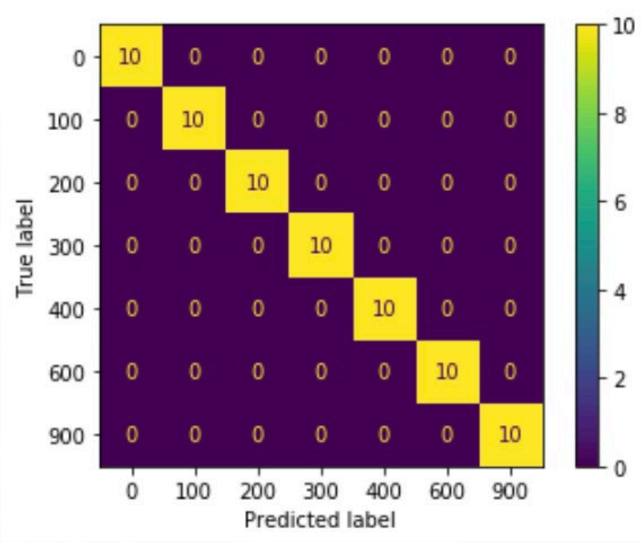

Confusion Matrix

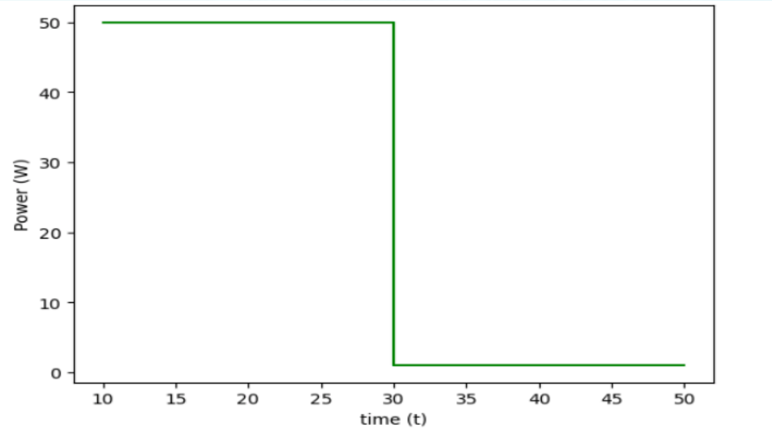

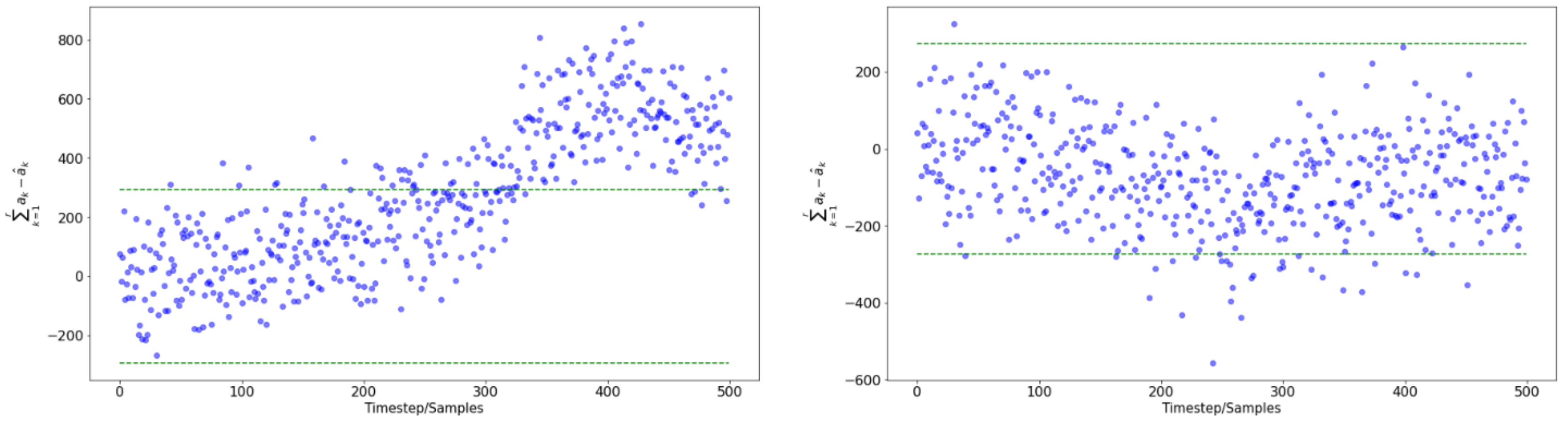

(a) Rank 10 model

(b) Rank 20 model

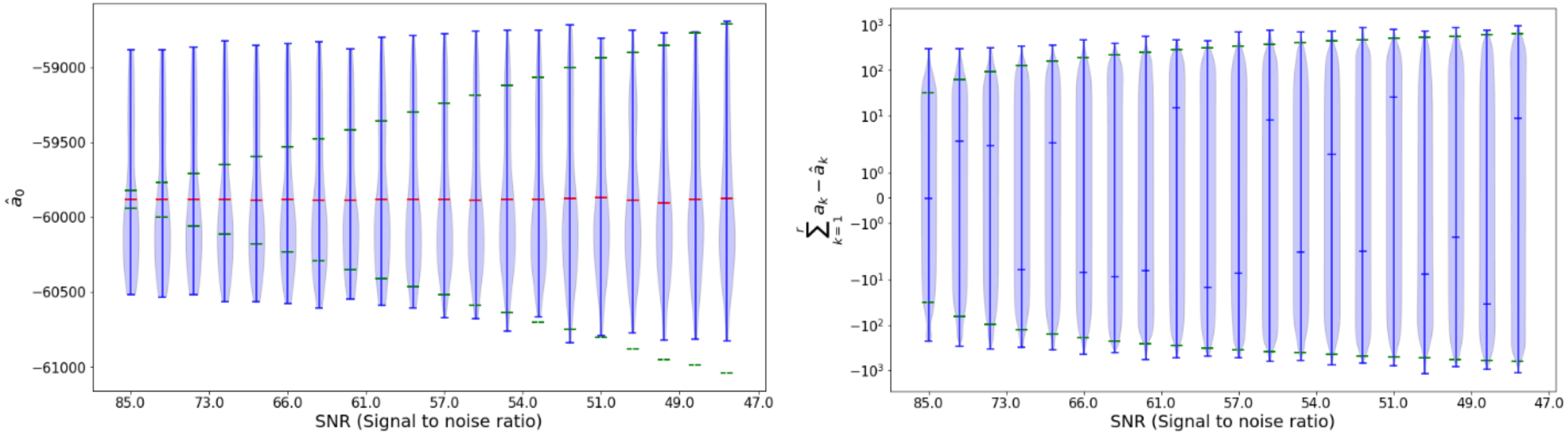

(c) Increasing uncertainty in estimation of $\hat{\mathbf{a}}_k$ with a decreasing SNR.

(d) Increase in estimation errors with a decreasing SNR.

a) Uncertainty estimation reveals that a rank 10 model is not sufficiently descriptive of dynamics after t =300 under sensor noise. The rank 20 approximation (b) is valid over a longer time horizon of 500s of test data. As the SNR decreases.

c,d) Estimation error is well captured by the standard deviation prediction as noise increases.